Economic valuation of subsurface water contributions to watershed ecosystem services using a fully-integrated groundwater–surface water model

Tariq Aziz[1,2,*], Steven K. Frey[1,3], David R. Lapen[4], Susan Preston[5], Hazen A. J. Russell[6], Omar Khader[1,7], Andre R. Erler[1], Edward A. Sudicky[1,3]

[1]Aquanty, 600 Weber St. N., Unit B, Waterloo, ON, N2V 1K4, Canada
[2]Ecohydrology Research Group, Water Institute and Department of Earth and Environmental Sciences, University of Waterloo, Waterloo, N2L 3G1, ON, Canada
[3]Department of Earth and Environmental Sciences, University of Waterloo, Waterloo, N2L 3G1, ON, Canada
[4]Agriculture and Agri-Food Canada, Ottawa Research and Development Centre, Ottawa, Ontario, Canada
[5]Environment and Climate Change Canada, Ottawa, Ontario, Canada
[6]Geological Survey of Canada, 601 Booth St., Ottawa, ON, K1A 0E8, Canada
[7]Department of Water and Water Structural Engineering, Zagazig University, AlSharqia, Egypt

*Correspondence to: Tariq Aziz (taziz@aquanty.com)

Abstract. Water is essential for all ecosystem services, yet a comprehensive assessment and valuation of total (overall) water contributions to ecosystem services production has never been attempted. Quantification of the many ecosystem services impacted by water demands an analytical approach that implicitly characterizes both subsurface and surface water resources; however, incorporating subsurface water into ecosystem services evaluation has until now remained elusive. In this study, a fully-integrated groundwater–surface water model—HydroGeoSphere (HGS)— is used to capture changes in subsurface water, surface water, and transpiration (green water use), and along with an economic valuation approach, forms the basis of an ecosystem services assessment for an 18-year period (2000-2017) in a mixed-use but a predominantly agricultural watershed in eastern Ontario, Canada. Using green water volumes generated by HGS and ecosystem services values as inputs, the marginal productivity of water is calculated to be \$0.26 per m^3 (in 2022 Canadian dollars). Results show maximum green water values during the driest years, with the extreme drought of 2012 being the highest at \$424.7 million. In contrast, the green water value in wetter years was as low as \$245.9 million, while the 18-year average was \$338.83 million. Because subsurface water is the sole contributor to the green water supply it plays a critical role in sustaining ecosystem services during drought conditions. This study provides new insight into the economic contributions of subsurface water and its role in sustaining ecosystem services during droughts, and puts forth improved methodology for watershed-based integrated management and valuation of ecosystem services.

1 Introduction

The role of subsurface water (groundwater and soil water in the vadose zone) in socio-economic development is widely acknowledged (Foster and Chilton, 2003); however, its ecological contributions are undervalued (Yang and Liu, 2020), despite being fundamental to the control of terrestrial ecological processes (Qiu et al., 2019). Subsurface water supports a potpourri of ecosystem services that range from provisioning to regulating, supporting, and cultural

36   services (Griebler and Avramov, 2015). While infiltration is a driver for subsurface water recharge, subsurface water

37   discharge is in-turn key for supporting terrestrial ecosystems (e.g., wetlands, forests, etc.) (Griebler and Avramov,

38   2015). Subsurface water provides a buffer against weather stressors on vegetation and aquatic ecosystems and helps

39   to maintain key processes that underpin ecosystem services (Qiu et al., 2019). To date, most ecosystem services

40   research has focused on aboveground factors and processes (e.g., land use change), and very little focus has been given

41   to the critical zone (e.g., shallow groundwater) and its influence on terrestrial ecosystem services (Richardson and

42   Kumar, 2017; Qiu et al., 2019). While some previous research (e.g., Booth et al., 2016; Li et al., 2014) has attempted

43   to link subsurface water with land cover, it reflects field scale, static environmental conditions (Qiu et al., 2019).

44   Given the difficulties with mapping large/watershed scale subsurface water resources, the contribution of subsurface

45   water towards terrestrial ecosystem services is not typically quantified, and the monetary/economic valuation of

46   subsurface water contribution to terrestrial ecosystem services is overlooked.

47   While hydrologic ecosystem services studies are common in the literature (Ochoa and Urbina-Cardona, 2017),

48   groundwater-focused ecosystem services assessments are rare. However, groundwater can be an important regulator

49   of watershed hydrologic behaviour and ecosystem health, especially in regions with a shallow water table, such as the

50   Laurentian Great Lakes Region (Neff et al., 2005; Kornelsen and Coulibaly, 2014). In addition, groundwater acts as

51   a source of soil water in shallow water table areas (Chen and Hu, 2004). The importance of groundwater has been

52   noted by Griebler and Avramov (2015) in their review of groundwater ecosystem services, where they highlight the

53   direct role it plays in supplying different types of ecosystem services (Millenium Ecosystem Assessment (MEA),

54   2005); and they stress the need for a better quantitative understanding of groundwater processes in order to protect

55   and manage groundwater ecosystem services. Furthermore, Mammola et al. (2019) emphasize that subterranean

56   ecosystems are largely being overlooked in conservation policies. Based on a preliminary assessment of all the regions

57   around the world where groundwater plays a critical role in ecosystem services, and considering that approximately

58   43 % of consumptive irrigation is sourced from groundwater (Siebert et al., 2010), one has to wonder if the lack of

59   focus on subsurface water ecosystem services is not due to lack of need, but in fact a lack of tools with which to

60   conduct the required analysis.

61   Hydrological models provide a convenient approach for characterizing water storages and fluxes over large spatial

62   scales. With groundwater ecosystem services' increasing role in policy-making (Honeck et al., 2021) and sustainable

63   groundwater resources management, new tools are required for the mapping process. At present, common modeling

64　tools available for ecosystem services mapping include relatively simple matrix models (i.e., Decsi et al., 2022), and

65　more complex models such as ARtificial Intelligence for Environment & Sustainability (ARIES) (Villa et al., 2021),

66　Co$ting Nature (Mulligan, 2015), Envision (Bolte, 2022), and Integrated Valuation of Ecosystem Services and

67　Tradeoffs (InVEST) (Natural Capital Project, 2022), with InVEST being by far the most prominent in the scientific

68　literature (Ochoa and Urbina-Cardona, 2017). However, ecosystem services specific models, such as the InVEST

69　Water Yield Model, have limited capability to simulate hydrological processes efficiently (Redhead et al. 2016),

70　because their hydrologic tools typically focus on one water compartment and/or are simplified to the point where

71　hydrologically mediated ecosystem services cannot be fully characterized (Dennedy-Frank et al., 2016; Vigerstol and

72　Aukema, 2011). Complete characterization of spatially and temporally varying water storages and fluxes that govern

73　ecosystem services over large spatial scales requires more sophisticated, process-based hydrological models (Sun et

74　al., 2017). Hence, models like SWAT (Arnold et al., 1998) and the Variable Infiltration Capacity (VIC) model (Liang

75　et al., 1994) have been used for hydrologic ecosystem services assessment, however even these models are unable to

76　simulate complex subsurface water movement and water exchanges between the surface and subsurface. Within the

77　hydrologic modelling community, it is acknowledged that structurally complex, fully-integrated subsurface–surface

78　water models are the current state-of-the-art for capturing the interplay between subsurface and surface water systems

79　(Barthel and Banzhaf, 2016; Berg and Sudicky, 2019), however, this class of models has not yet been applied towards

80　ecosystem services valuation.

81　A key hydrologic process influencing ecosystem services is evapotranspiration, which can be closely related to the

82　availability of shallow groundwater (Jin et al., 2017; Condon et al., 2020). Evapotranspiration is a fraction of rainfall

83　that eventually returns to the atmosphere through evaporation and transpiration, which represent large fluxes of both

84　water and energy across the land surface–atmosphere boundary (Tan et al., 2021). While evaporation is often perceived

85　as a water loss, transpiration is an essential process for sustaining ecosystems and providing terrestrial ecosystem

86　services (An and Verhoeven, 2019). Transpiration is also called productive green water—the fraction of the rainfall

87　on the land that eventually returns to the atmosphere via plants. It is a source of nutrition for vegetation/ecosystems

88　(Casagrande et al., 2021), and plays a key role in the production of biomass and ecosystem services (Zisopoulou et

89　al., 2022; Schyns et al., 2019). Green water is essential for functioning and growth of ecosystems, and thus supports

90　and maintains terrestrial ecosystem services (Lowe et al., 2022). Hence, transpiration serves as a key driver in

91 providing ecosystem services (Liu and El-Kassaby, 2017), and is a fundamental process by which to model/map

92 terrestrial ecosystem services production.

93 Changes in evapotranspiration rates can influence water availability and ecosystem health at a watershed scale (Zhao

94 et al., 2022). Thus, subsurface water availability is an important when considering ecosystem function and ecosystem

95 services. Under drought conditions, subsurface water can become critically important for sustaining transpiration

96 (Condon et al., 2020), and hence, mapping the subsurface water - transpiration connection is imperative for sustainable

97 water and ecosystem services management (Yang et al., 2015). In cases where growing climate variability is expected

98 to result in increasingly erratic precipitation patterns, capturing these connections becomes even more important

99 (Taylor et al., 2013). While a few common hydrological models can weakly capture the subsurface water dynamics

100 and subsurface-surface water interactions (Clark et al., 2015), fully integrated subsurface-surface hydrologic models

101 can dynamically resolve water exchange between groundwater, surface water, and soil moisture, and evaporation and

102 transpiration fluxes with much higher levels of spatial and temporal fidelity. Benchmarking studies have been

103 conducted wherein the most common subsurface-surface hydrologic models have been described in detail, and their

104 simulation behavior compared (Maxwell et al., 2014; Kollet et al., 2016).

105 In this study, we introduce the HydroGeoSphere (HGS) fully-integrated subsurface–surface water model (Aquanty,

106 2021; Brunner and Simmons, 2012) as a tool for mapping key hydrological fluxes and water storage fluctuations, and

107 quantifying subsurface water contributions to terrestrial ecosystem services at the watershed scale (~4000 km^2). The

108 results from the HGS modelling are extended to an economic valuation of water contributions to ecosystem services.

109 Until now, fully-integrated subsurface-surface models such as HGS have not been widely demonstrated in the

110 scientific literature as tools for modeling ecosystem services, while at the same time, the economic value of subsurface

111 water has been overlooked in ecosystem services valuation assessments. Accordingly, the study herein is a novel

112 contribution towards improving our understanding of overall hydrologic contributions to ecosystem services.

113 Furthermore, using the HGS model outputs to support the economic valuation of subsurface water contributions to

114 transpiration, and subsequently to terrestrial ecosystem services, is also novel. Hence, this work provides an important

115 advancement to the science of ecosystem service valuation in terms of conceptual, methodological, and quantitative

116 understanding.

2 Materials and Methods

2.1 Study Area

This study focuses on the South Nation watershed (SNW), located in eastern Ontario, Canada, with an area of approximately 3,830 km^2 (Fig. 1). The SNW is relatively flat, with approximately 100 m of vertical relief in the land surface. It is primarily an agriculture-focused watershed, with relatively low population density, where for example the towns of Casselman, Russell, and Winchester (population centres within the SNW) have respective populations of 3,548, 16,520 and 2,394 based on the 2016 Canada census. The eastern flank of the city of Ottawa encroaches on the Northwest corner of the watershed. The SNW surface water flow network is approximately 6,489 km long and consists of 1,606 km of Strahler order 3+ (relatively large), 1,548 km of Strahler order 2, and 3,335 km of Strahler order 1 (smallest) river and stream features (Fig. 2A). Many of the low order features are either manmade agricultural drainage ditches or straightened natural watercourses designed to drain the agricultural landscape.

Soil drainage conditions across the watershed are primarily imperfect, poor, or very poor (Fig. 3A), although some disconnected pockets are considered well drained (Soil Landscapes of Canada Working Group, 2010). The wide extent of poorly drained soils in the SNW is an integral reason for the intensive land drainage activities. Tile drainage is employed in approximately 960 km^2 (or 25 %) of the watershed to enhance agricultural productivity and to facilitate cropping activities (Fig. 4A). Across most of the SNW the soils are primarily underlain by glacial, fluvial, and colluvial Quaternary deposits (Ontario Geological Survey, 2010). These sediments are composed of sand, silt, clay, gravel, and glacial till, and range in thickness from 0 m to approximately 90 m across the watershed. Eight soils have been identified in the SNW (Soil Landscapes of Canada Working Group, 2010), mainly composed of clay loam and sandy loam textures (Fig. 3A(a)). Localized incised bedrock channels and Quaternary esker deposits are important sources of groundwater for both ecological function and human/livestock supply, and most of the rural residents in the SNW rely on groundwater for domestic and farm use.

The SNW is characterized by relatively wet temperate climate with cold winters and warm summers. The annual average temperature is just over 5 C, with average summer highs reaching 26°C in July and average winter lows reaching -14°C in January (https://climate.weather.gc.ca/climate_normals). Present day landcover (Fig. 1) consists of 38% cropland, 29% forest, 20% grassland, 7% urban, 5% wetland, and 1% water. Within the SNW, grasslands support the extensive dairy industry, which plays an important role in the local economy.

5

144
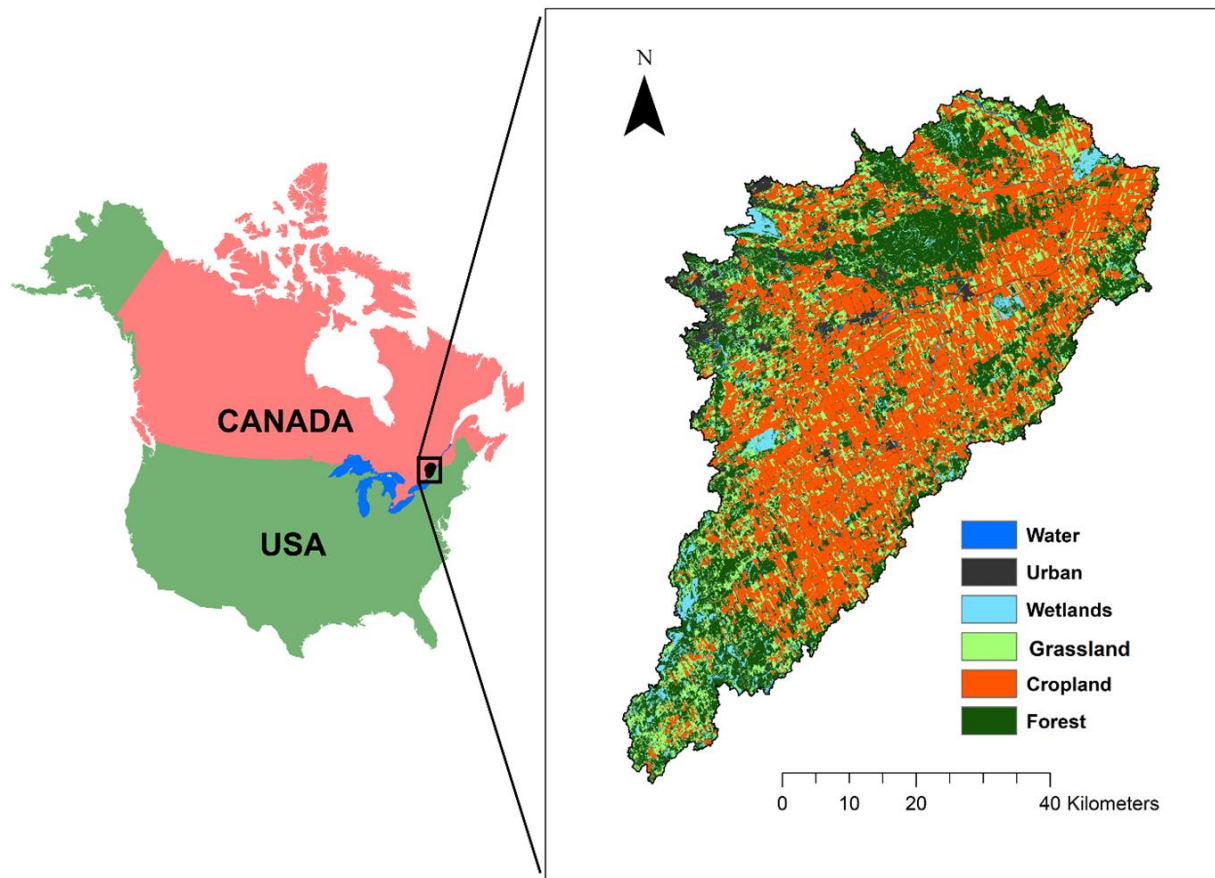
Figure 1: Location of the South Nation Watershed (SNW) in North America. The inset figure (right) shows the land use distribution across the SNW.

2.2 Water balance quantification with HydroGeoSphere (HGS)

The water balance strongly influences ecosystem functions and the associated ecosystem services, as it governs both abiotic and biotic processes occurring within ecosystems (Mercado-bettín et al., 2019). Consequently, evaluating the role of water towards ecosystem services supply necessitates an analysis capable of water balance partitioning (i.e., disaggregation of the water balance into its fundamental components such as precipitation, subsurface evaporation, transpiration, surface and subsurface storages) (Casagrande et al., 2021). As HGS is a dynamic fully-integrated subsurface–surface hydrologic model, it generates time varying simulation outputs for all components of the terrestrial hydrologic cycle (Fig. 2), thus alleviating a common limitation of ecosystem services models in that they do not account for transient behavior (Vigerstol and Aukema, 2011). HGS employs a physically based approach to simulate

water movement and the partitioning of precipitation input into surface runoff, streamflow, evaporation, transpiration, groundwater recharge, as well as groundwater discharge into surface water bodies like rivers and lakes (Brunner and Simmons, 2012). Furthermore, HGS outputs can also be generated for the entire model domain (i.e., the watershed) or refined for smaller spatial scales such as subwatersheds, with the downscale limit being that of an individual finite element within the finite element mesh (FEM).
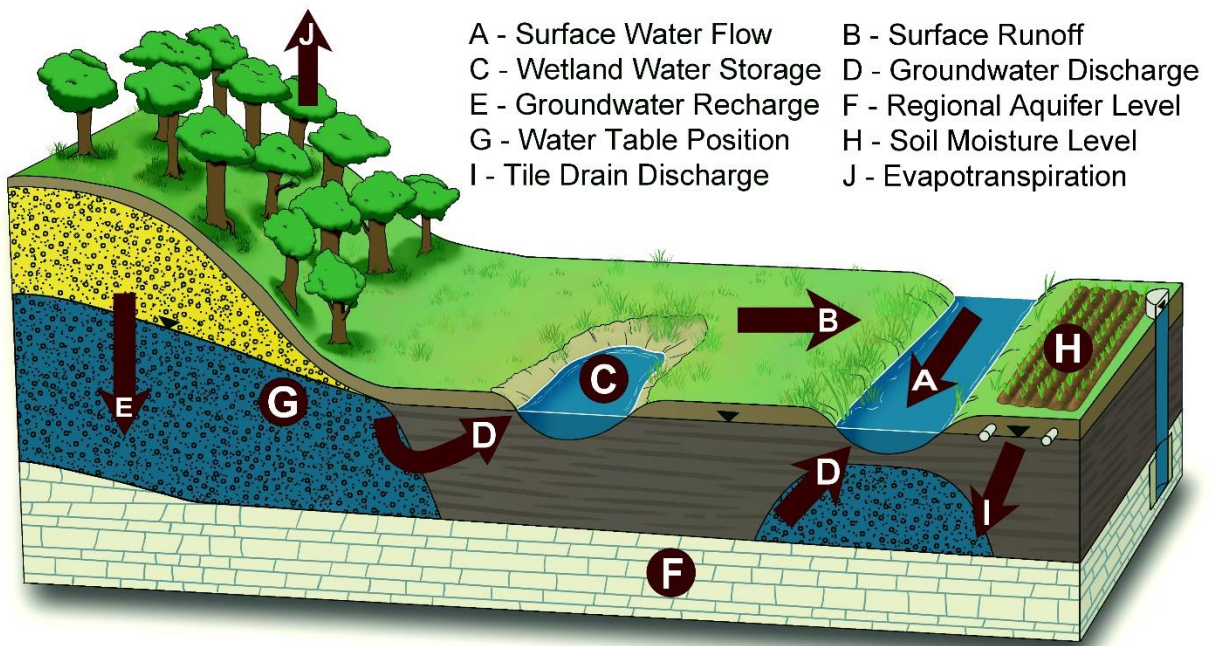
Figure 2: Key components of the terrestrial hydrological cycle captured in HGS models over a range of spatial scales.

It should be noted that the fidelity of the HGS outputs are also dependent on the model scale, with large scale models generally having lower spatial resolution than small scale models as a result of computational constraints, and in some cases, data constraints. For example, a model of a 766,000 km^2 river basin (e.g., Xu et al., 2021a)) is best suited to answer big picture questions (i.e., basin water balance, regional groundwater), while a model built at similar scale to the SNW (e.g., Frey et al., 2021)) can be used to address questions pertaining to localized processes (i.e., individual wetland influences, groundwater recharge and discharge patterns, aquifer conditions, and soil moisture conditions). If even more localized insights are required, HGS models can be constructed for field or plot scale domains (up to approximately 10 km^2), where highly detailed questions pertaining to things such as riparian zones, soil structure, manure application, and tile drainage influences on both water quantity and quality can be evaluated (Fig. 2). Thus,

173   HGS is a scalable and robust model for ecosystem services analysis across a range of different spatial scales and

174   different levels of hydrologic process detail. For the SNW, HGS is used to simulate watershed surface water outflow,

175   transpiration (green water), subsurface water storage, and land surface water storage (reflecting water held in wetlands

176   and reservoirs) using the model construction framework presented in Frey et al. (2021).

177   **2.2.1 Model construction**

178   **2.2.1.1 Finite Element Mesh (FEM)**

179   The HGS model utilizes a 3-D unstructured FEM that extends across the full 3830 km^2 area of the SNW. The 1-D

180   river/stream channel features, 2-D overland flow domain (reflecting land surface topography), and 3-D subsurface

181   flow domain (reflecting hydrostratigraphy) all share the same mesh geometry, with the 1-D and 2-D domains sharing

182   common coordinates with the 3-D domain across the top surface of the model. The FEM for the SNW model resolves

183   all Strahler 2+ stream/river features as mesh discretization control lines, with element edge length maintained at 100

184   m, while away from the control lines the element edge lengths extend up to 300 m. The FEM contains layer surfaces

185   that correspond to hydrostratigraphic surfaces, with each individual layer consisting of 171,609 finite elements.

186   Accordingly, over the eight model surfaces (seven subsurface layers); the FEM contains 1,201,263 3-D finite elements.

187   **2.2.1.2 Hydrostratigraphy**

188   The seven subsurface layers represent (from the top down) three soil layers, three Quaternary hydrostratigraphic

189   layers, and one bedrock layer. The soil layers extend from 0–0.25 m, 0.25–0.5 m, and 0.5–1 m depth relative to the

190   top surface, which is defined with the Ontario Integrated Hydrology Data digital elevation model

191   (https://geohub.lio.gov.on.ca/maps/mnrf::ontario-integrated-hydrology-oih-data/about). The hydraulic properties for

192   the soil layers vary spatially according to the soil polygons defined in the Soil Landscapes of Canada (SLC, Soil

193   Landscapes of Canada Working Group, 2010), and are defined in two steps as follows: (1) properties extracted from

194   SLC are used in conjunction with the Rosetta pedotransfer functions (Schaap et al., 2001) to obtain estimates for

195   hydraulic conductivity, water retention and relative permeability, residual saturation, and porosity parameters, and (2)

196   hydraulic conductivity, water retention and relative permeability parameters are subsequently tuned during model

197   calibration. The three Quaternary layers are of variable thickness, where the interface surfaces represent lithology

198   contrasts derived from a simplified version of the 3-D geological model produced for the SNW by Logan et al. (2009).

199   Hydraulic properties for the Quaternary materials are assigned based on lithology. Underlying the Quaternary layers

200   is a single hydrostratigraphic layer with uniform hydraulic conductivity representative of the Phanerozoic bedrock.

201   When assembled, the model layers depict a 3-D subsurface realization of the SNW hydrostratigraphy (Fig. 3).

202
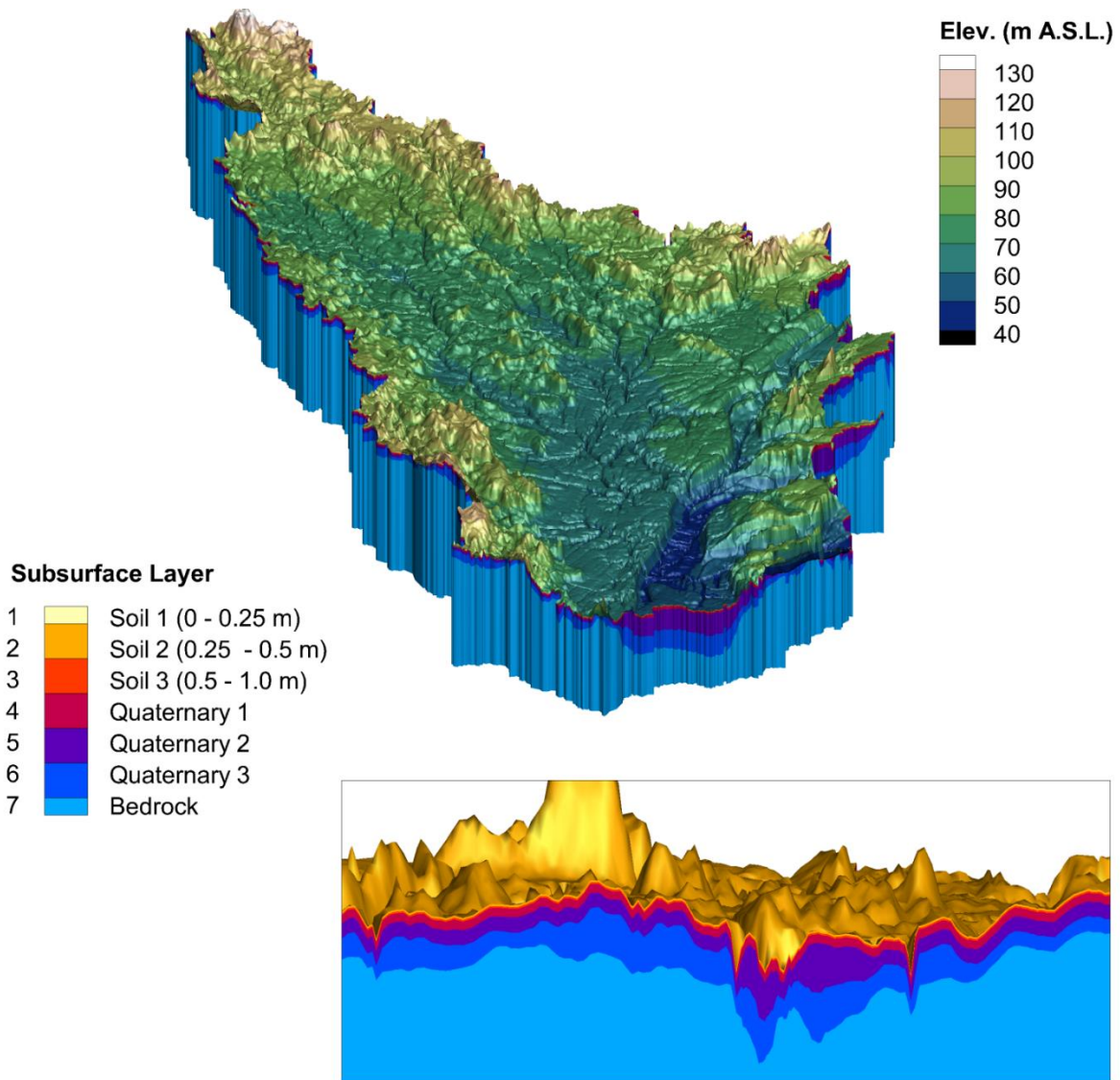
Figure 3:   Three-dimensional perspective of the South Nation HydroGeoSphere model, and the hydrostratigraphic layering (inset). Note the 100x vertical exaggeration.

2.2.1.3 Land Surface Configuration

The land surface in the HGS model represents land cover distribution defined by the gridded, 30 m resolution, 2017 Annual Crop Inventory dataset (Agriculture and Agri-Food Canada, 2022) simplified to six categories (water, urban, wetland, grassland, cropland, and forest). Root depth for the cropland (1 m), forest (2.9 m), wetland (1 m), grassland (2.1 m), and urban (1 m) landcovers was held static over the simulation interval. Spatially distributed leaf area index (LAI) is a transient parameter defined with the 8-day composite, 500 m resolution MOD15A2H v006 data product

9

211 (Myneni et al., 2021). Each landcover category utilizes a unique surface roughness (Manning's *n* coefficient) value,

212 ranging from 0.001 (urban) to 0.03 s/m$^{1/3}$ (forest). Land cover properties, as well as subsurface hydraulic properties,

213 were mapped into the HGS model's unstructured FEM using a dominant component approach, such that when two or

214 more property classes exist within the input data set for a single finite element, the majority class is represented.

215 **2.2.1.4 Climatology**

216 Time-varying and spatially distributed climate data with daily temporal resolution liquid water influx (LWF) and

217 potential evapotranspiration (PET) is used to force the HGS model for the 2000 to 2018 simulation interval. LWF is

218 derived from precipitation obtained from McKenney et al. (2011) in combination with snow water equivalent (SWE)

219 estimates from the ERA5-Land land-surface reanalysis (Muñoz-Sabater et al., 2021), where LWF is the sum of liquid

220 precipitation (rain) and snowmelt (daily changes in SWE).

221 Potential evapotranspiration primarily depends on the surface radiation budget, temperature, humidity, and near-

222 surface wind speed (Allen et al., 1998); however, of these variables, only minimum and maximum temperature are

223 readily available for the full SNW. Hence, PET forcing for the SNW model is calculated with the Hogg method (Hogg,

224 1997), which is consistent with Erler et al. (2019) and Xu et al. (2021), who both reported good agreement with the

225 observed water balance in the Great Lakes region when using the Hogg method. The Hogg method is based on the

226 FAO Penman-Monteith approach (Allen et al. 1998) with a simplification that involves the radiation budget and

227 humidity approximated as a function of daily minimum and maximum temperature, and wind speed assumed to be

228 constant.

229 **2.2.2 Model Performance Evaluation**

230 The SNW HGS model was run continuously from 2000–2017 with daily temporal resolution climate forcing, and

231 simulation performance is evaluated using observed surface water flow rates and groundwater levels. The observation

232 data is derived from daily temporal resolution surface water flow monitoring conducted at nine Water Survey of

233 Canada (WSC) hydrometric stations (Figure 4a) and groundwater level data from 10 Provincial Groundwater

234 Monitoring Network wells that was collected hourly but aggregated into daily average values (Figure 4b). The Nash-

235 Sutcliffe Efficiency (NSE) and Percent Bias (Pbias) metrics (Moriasi et al., 2007) are used to evaluate surface water

236 flow simulation performance, while the coefficient of determination (R^2) and root mean square error (RMSE) is used

237 to evaluate groundwater simulation performance. It should be noted that groundwater pumping is not represented in

238   the model as it is deemed to be a very minor component of the overall water balance, and because it is extremely

239   difficult to characterize and simulate at the scale of the SNW.
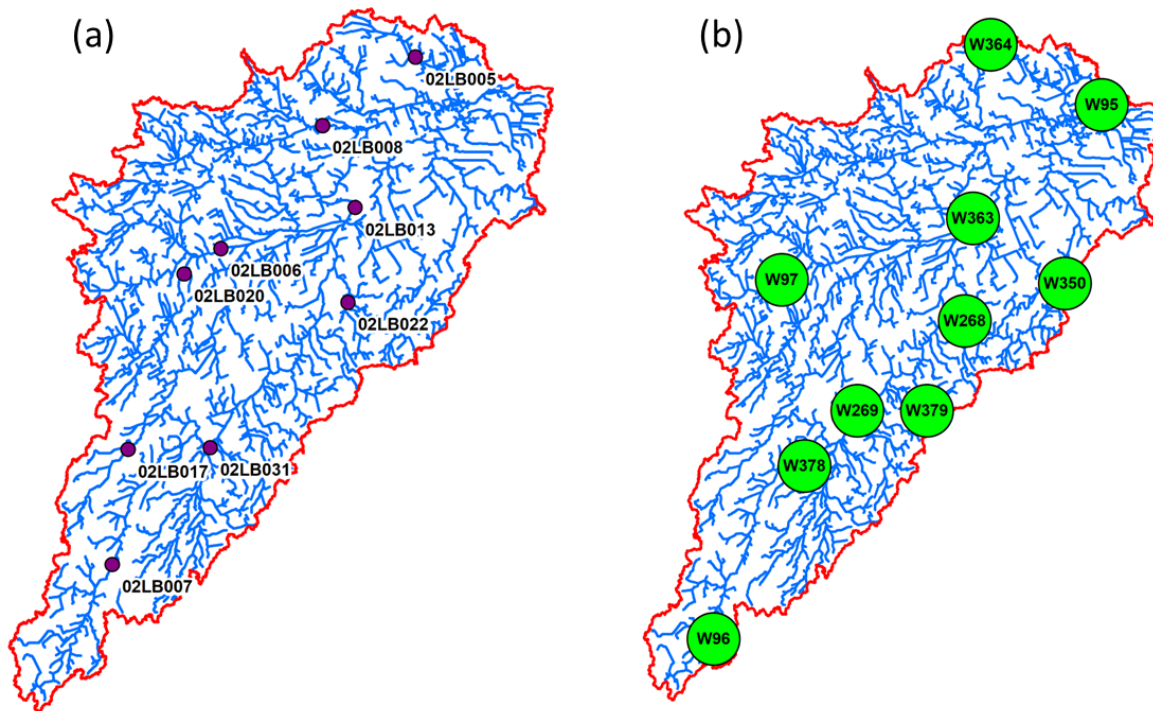
240

241   **Figure 4. Distribution of (a) Water Survey of Canada surface water flow gauges, and (b) Provincial**

242   **Groundwater Monitoring Network wells across the South Nation watershed.**

243   **2.3 Ecosystem services water productivity**

244   The benefit transfer method is used to derive the unit values of ecosystems in the SNW. The benefit transfer method,

245   which is a widely used technique for assessing the economic value of ecosystem services, relies on secondary data

246   obtained through the implementation of various other economic valuation methods (Aziz, 2021). A study conducted

247   approximately 65 km from the SNW in the Ottawa-Gatineau region, by L'Ecuyer-Sauvageau et al. (2021), assembles

248   the values for 13 ecosystem services: agricultural services, global climate regulation, air quality, water provision,

249   waste treatment, erosion control, pollination, habitat for biodiversity, natural hazard prevention, pest management,

250   nutrient cycling, landscape aesthetics, and recreational activities. Because of data limitations, raw material, genetic

251   diversity, spiritual, cultural and heritage identity ecosystem services are excluded from the L'Ecuyer-Sauvageau et al.

252   (2021) analysis. These unit values have been correspondingly generated by major ecosystems using market price,

253   replacement cost, and benefit transfer methods. The unit values for ecosystem services are based on similarities in

254   ecologic and socio-economic conditions between the studied and policy sites, and converted using the purchasing

255   power parity (L'Ecuyer-Sauvageau et al., 2021). After adjusting these values for inflation, the value of ecosystem

256   services in the SNW is calculated using the following equation.

257    $$EV_t = \sum_{k=1}^{n}(A_k \times UV_k) * VI \qquad (1)$$

258   EV_t = Value of ecosystem services for year t

259   A_k = Area of land use k

260   UV_k = Unit value of ecosystem services for land use k

261   VI = Vegetation indicator, a ratio of yearly to average net primary production (NPP) = NPP_{year}/NPP_{mean}

262   We use net primary production as an indicator to characterize the vegetation vigor (Xu et al., 2012) and to adjust the

263   values of ecosystem services over time in the SNW. The relative vegetation indicator (VI) is the ratio of yearly NPP

264   and the mean NPP over the selected period.   The Moderate Resolution Imaging Spectroradiometer (MODIS)

265   (https://appeears.earthdatacloud.nasa.gov/) NPP data (at 500m resolution) for the 2000 to 2017 study period is used.

266   Using the ArcGIS Spatial Analyst Toolbox, yearly mean NPP values are calculated (Table 2). The average ecosystem

267   services water productivity is then calculated using ecosystem services values and productive green water volumes

268   (i.e., transpiration) in equation 2:

269    $$V_W = (EV_t)/(X_w) \qquad (2)$$

270   V_w is the average product of water (\$ per m^3), X_w is the total volume of water transpired (or productive green water

271   volume) in a year 't'.

272   **2.4 Valuation of subsurface water contribution towards ecosystem services supply**

273   A water production function is developed using economic values of the watershed for ecosystem services supply over

274   the 18-year study period and corresponding volumes of green water consumption. Because ecosystem services value

275   is proportional to biomass production (Costanza et al., 1998), the values are modified over time using relative changes

276   in ecosystems biomass in the watershed (Xu and Xiao, 2022). The slope of the production function represents the

277   ecosystem services marginal water productivity (MP_w). HGS model outputs capture the volume of subsurface water

278   contributing to transpiration. Using the volumes of subsurface water consumed for transpiration and MP_w, the

279   economic value of green water from the storages used for ecosystem services supply is calculated (Eq.3).

280    $$V_i = X_{wi} * MP_w \qquad (3)$$

281   Where V_i is the value of water storage i towards ecosystem services supply, X_{wi} is the volume of water storage i used

282   towards green water supply, and MP_w is the marginal productivity of water.

283   **3 Results**

284   **3.1 HGS outputs**

285   For the 2000 to 2017 simulation interval, the HGS model reproduces surface water flow rates at the nine WSC

286   hydrometric stations across the SNW with good accuracy per the interpretation guidance provided by Moriasi et al.

287   (2007). Based on daily evaluation frequency, NSE at the individual gauge stations ranges from 0.59 to 0.70, with a

288   mean of 0.66; while PBias ranged from -17.4 % to 17.1 %, with a mean of 3.9 % (Fig. 5). Groundwater levels were

289   also reproduced across the SNW with reasonable accuracy for the 2000 to 2017 interval. The R^2 between simulated

290   and observed water levels in the 10 observation wells is 0.98, with the simulated values having a mean value 2.8 m

291   higher than the observed values. Groundwater simulation performance at the individual wells is presented in Table 1.

292   HGS outputs (Fig. 6) also include total watershed surface water outflow, ET_a rates (based on subsurface transpiration

293   and evaporation, surface evaporation and canopy evaporation), subsurface water storage (groundwater storage plus

294   soil moisture storage) and land surface water storage. During the simulation period, transpiration accounts for a

295   substantial proportion of ET_a, ranging from 45% to 65% (Table A1). Consequently, it emerges as the dominant process

296   contributing to the overall ET_a. As evident in Fig. 6, water storage volumes fluctuate over inter- and intra-annual time

297   frames, with the most notable decline in storage aligned closely with the drought in 2012.

298
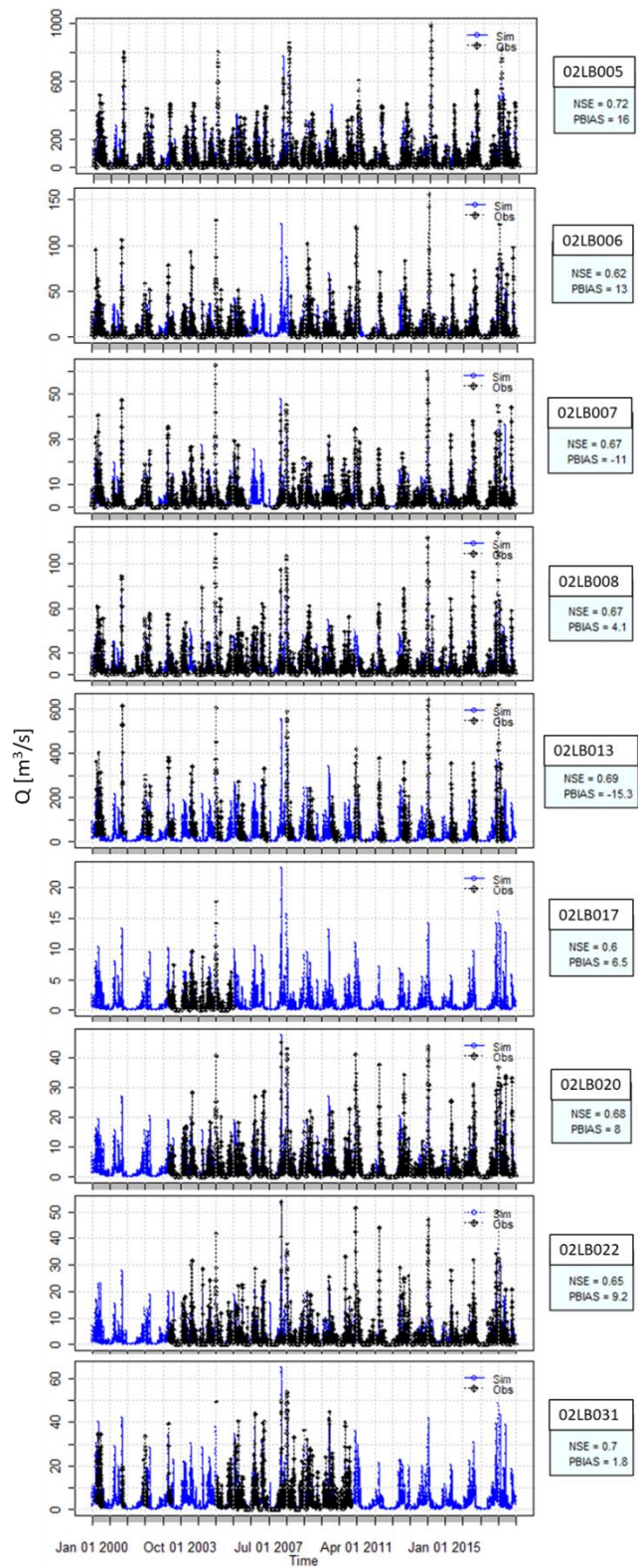
Figure 5. Simulated vs. observed surface water flow rates at the nine Water Survey of Canada (WSC) flow gauges incorporated into the model calibration process, along with Nash-Sutcliffe Model Efficiency (NSE) and Percent Bias (PBias in %) performance metrics. Note that not all gauges have a full data record over the 18-year simulation interval.

14

302 **Table 1. For the 10 monitoring well locations, observed vs. simulated average groundwater head, and root mean square**
303 **error between daily temporal resolution observed and simulated head, over the 2000 – 2017 simulation interval.**

Well	Observed Average Head (mASL)	Simulated Average Head (mASL)	RMSE (m)
95	48.2	62.0	13.8
96	99.1	99.1	0.8
97	84.9	86.9	2.1
268	72.4	72.3	0.5
269	68.4	70.9	2.7
350	111.3	109.5	2.1
363	57.4	61.6	4.2
364	43.2	50.3	7.2
378	74.7	77.0	2.4
379	89.4	87.4	1.9

304

(a)

(b)

(c)

(d)
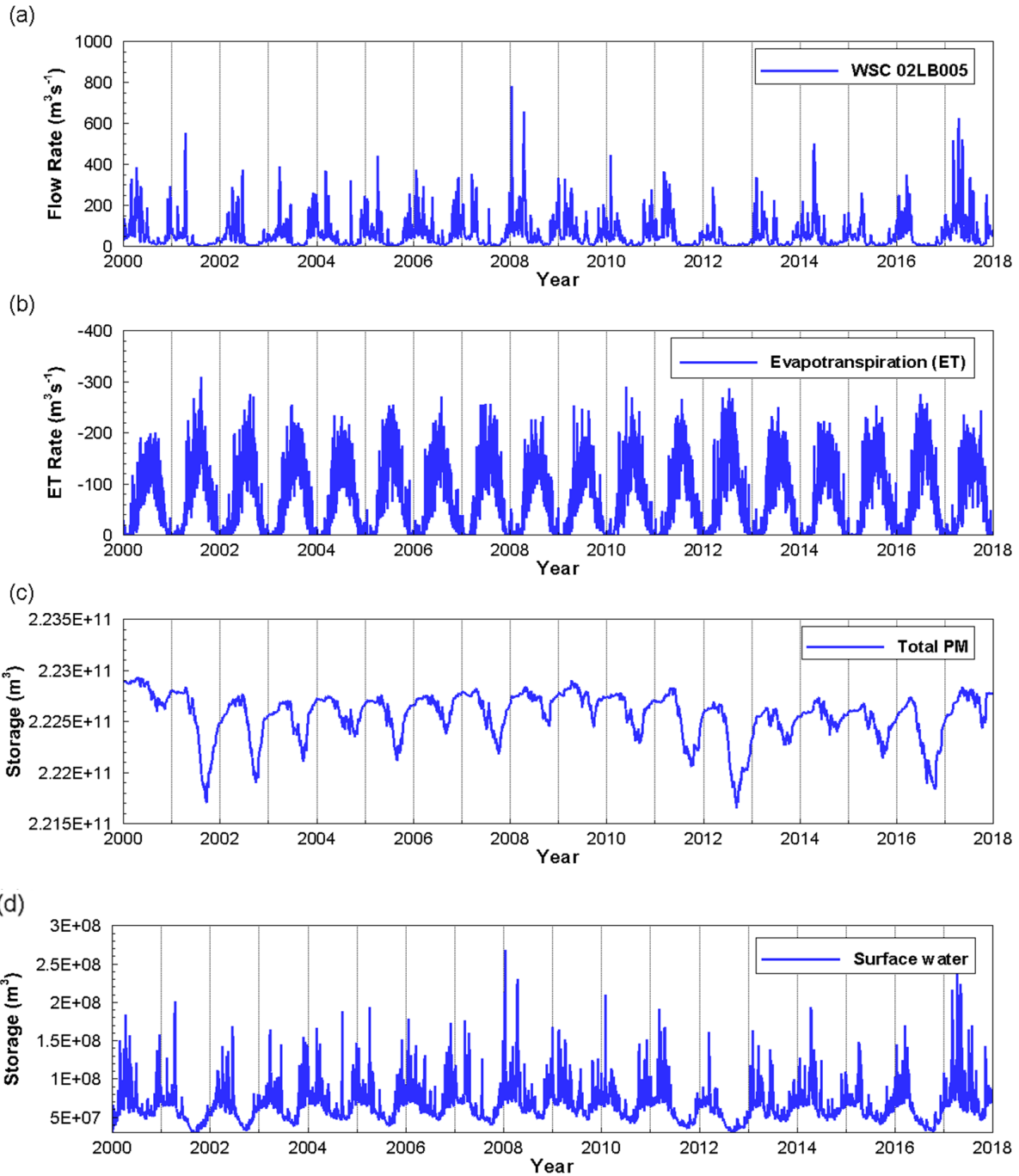
305

306 **Figure 6: Time series outputs from the South Nation watershed HydroGeoSphere (HGS) simulation over the**

307 **2000-to-2017-time interval. (a) stream flow at the furthest downstream hydrometric station, (b) watershed**

308 **evapotranspiration, (c) watershed subsurface water storage, and (d) watershed land surface water storage.**

309 The HGS output was generated at variable time steps that were each no larger than 1 day, and then aggregated to

310 yearly values for use in the ecosystem services assessment (Table 1A). Annual deviations from the long term mean,

311 for ET_a, transpiration, total precipitation, and surface and subsurface water storage, are presented in Fig. 7. In the

312   context of subsequent analysis and discussion, it should be noted that the drought year of 2012 exhibits the highest

313   ET_a and transpiration, lowest precipitation, and large drops in both subsurface and surface water storage.

314
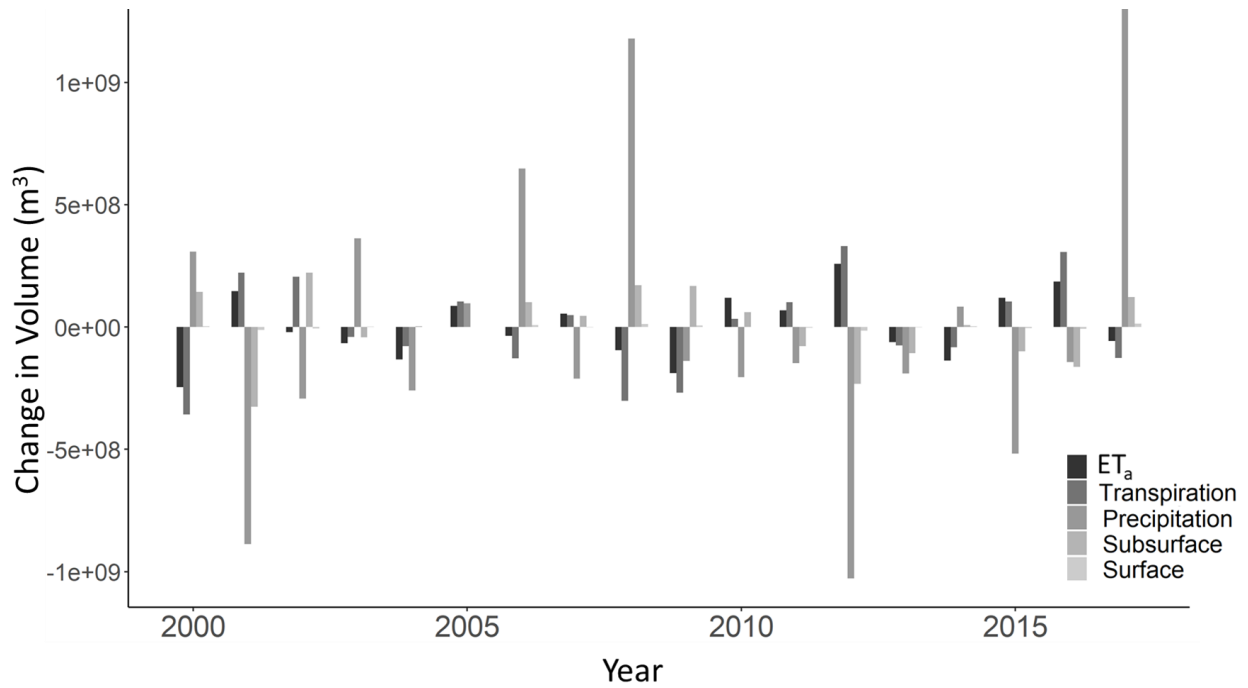
Figure 7: Annual deviation from the long term (2000-2017) mean evapotranspiration, transpiration, precipitation, and subsurface and surface water storages.

317   **3.2 Valuation of ecosystem services, and average and marginal water productivity**

318   **Table 2: Land use types and unit values for the SNW.**

| Land Use	Area (hectare)	Unit value ($/hectare/year)
Water	1,299	165
Urban	25,734	1,177
Wetlands	16,709	71,273
Grasslands	7,6961	4,152
Croplands	154,810	1,666
Forest	107,470	4,993

319

320   Using unit values for the major land use types in the SNW (Table 2) and land use area, total value of the 13 ecosystem

321   services under consideration is $2.33 billion per year (in CAD 2022) prior to further annual modifications based on

17

322   the vegetation indicator (Eq. 1). The estimates for average product of water are point estimates based on the value of

323   ecosystem services and productive green water volume (i.e., transpiration) for the corresponding year. Annual NPP

324   data, ES values, transpiration volume, and average water product in the SNW are given in Table 3.

325   **Table 3: Mean Net Primary Production (NPP), ecosystem services (ES) values, transpiration volume, and**

326   **average product of water for the SNW over the 18-year study interval.**

| Year	Mean NPP (Kg C/m^2/year)	ES Value (x10^9 \$/year)	Transpiration (x10^9 m^3)	Average product of water (\$/m^3)
2000	0.59	2.26	0.95	2.39
2001	0.65	2.49	1.53	1.63
2002	0.6	2.30	1.51	1.52
2003	0.6	2.30	1.26	1.82
2004	0.62	2.37	1.22	1.94
2005	0.63	2.41	1.41	1.71
2006	0.58	2.22	1.18	1.89
2007	0.63	2.41	1.35	1.78
2008	0.6	2.30	1.00	2.29
2009	0.58	2.22	1.03	2.14
2010	0.64	2.45	1.34	1.83
2011	0.6	2.30	1.40	1.63
2012	0.63	2.41	1.63	1.48
2013	0.58	2.22	1.23	1.81
2014	0.59	2.26	1.22	1.85
2015	0.65	2.49	1.41	1.77
2016	0.6	2.30	1.61	1.43
2017	0.59	2.26	1.18	1.92

327

328   For the ecosystem services marginal water productivity, a production function is developed using transpiration and

329   ES values for the SNW (Fig. 8) and the slope of the function equates to the marginal productivity of water, which is

330   \$0.26/m^3.

$$y = 2 \times 10^{+9} + 0.26\, x$$
$$R^2 = 0.32$$

331
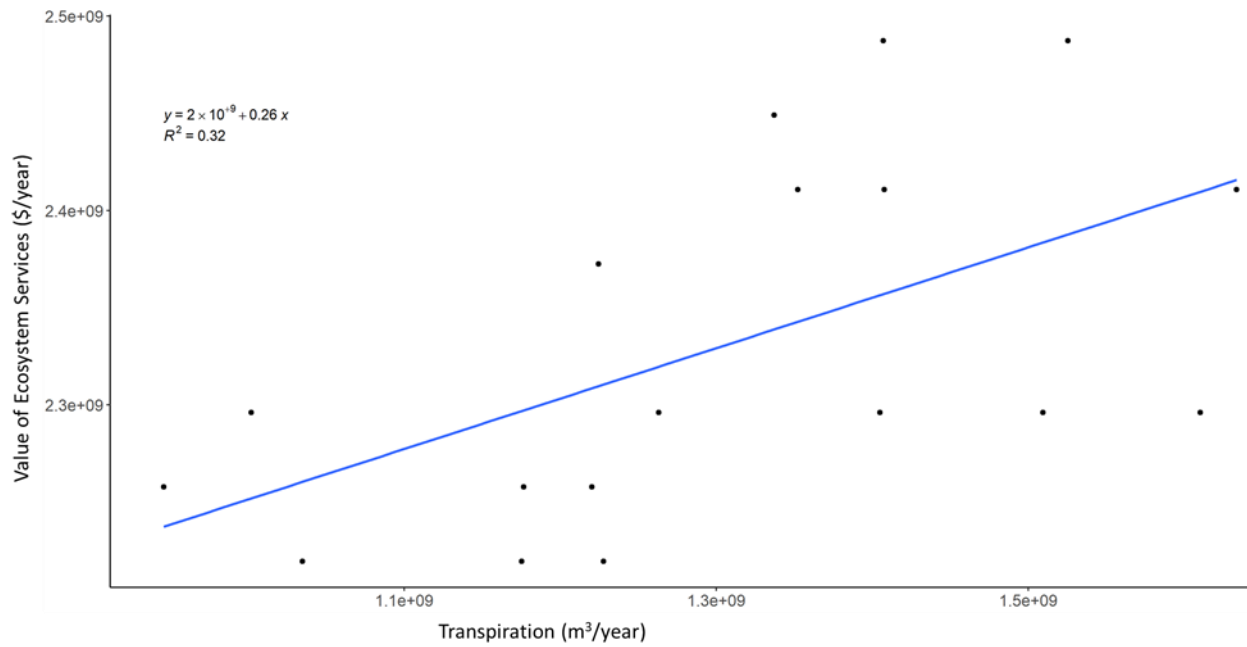
**Figure 8: Ecosystem services water production function for the South Nation Watershed.**

To assess the contribution of subsurface water towards ecosystem services, the average ecosystem services water productivity at the watershed scale is calculated (Table 3). The average product of water over the 18 year study interval ranges from \$1.43-2.39 per m^3 (Fig. 9). During the drought years (2001-2002, 2012 and 2016), the average product of water declines to local minima. This is because the average product depicts water use efficiency, with the highest value observed for year 2000 indicating that hydrologic conditions favoured the maximum production of ecosystem services with the lowest water consumption in that year.

339
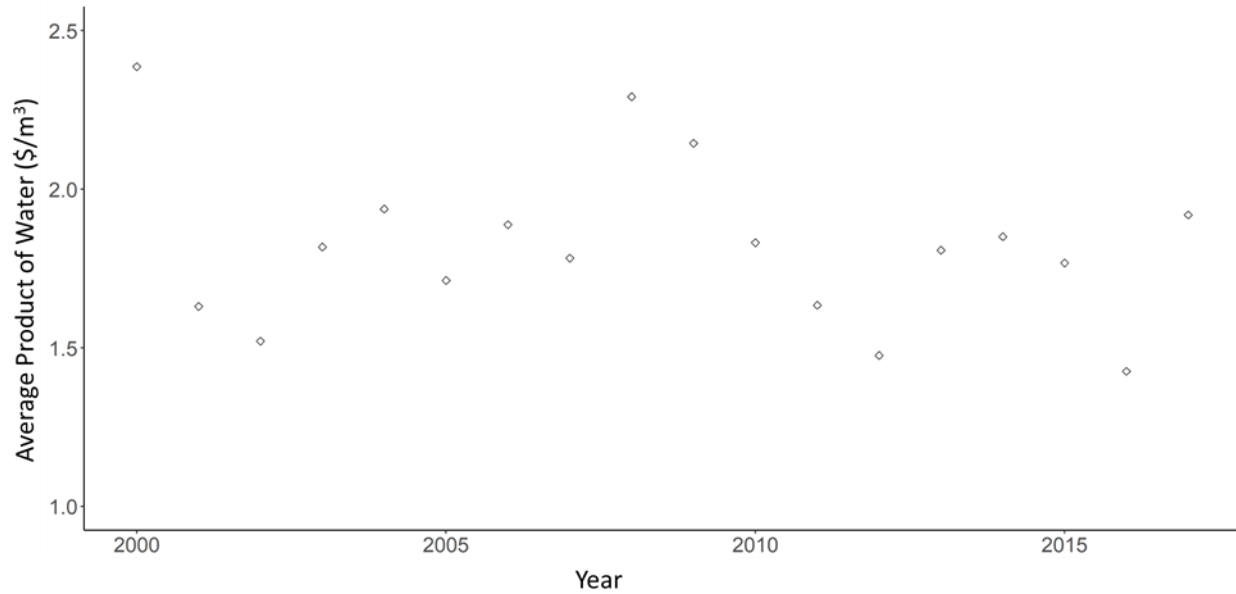
Figure 9: Average annual product of water for ecosystem services in the SNW over the 18-year study period.

3.3 Valuation of green, subsurface, and surface waters

Using the marginal water productivity and transpiration in the SNW, the value of green water over the study period was calculated (Fig. 10). The annual values range from $245.9 (year 2000) to $424.7 (year 2012) million per year, with an overall average of $338.83 million. In general, there is a strong inverse correlation between total annual precipitation and green water value, with an R^2 of 0.45 (p <0.0001).

346
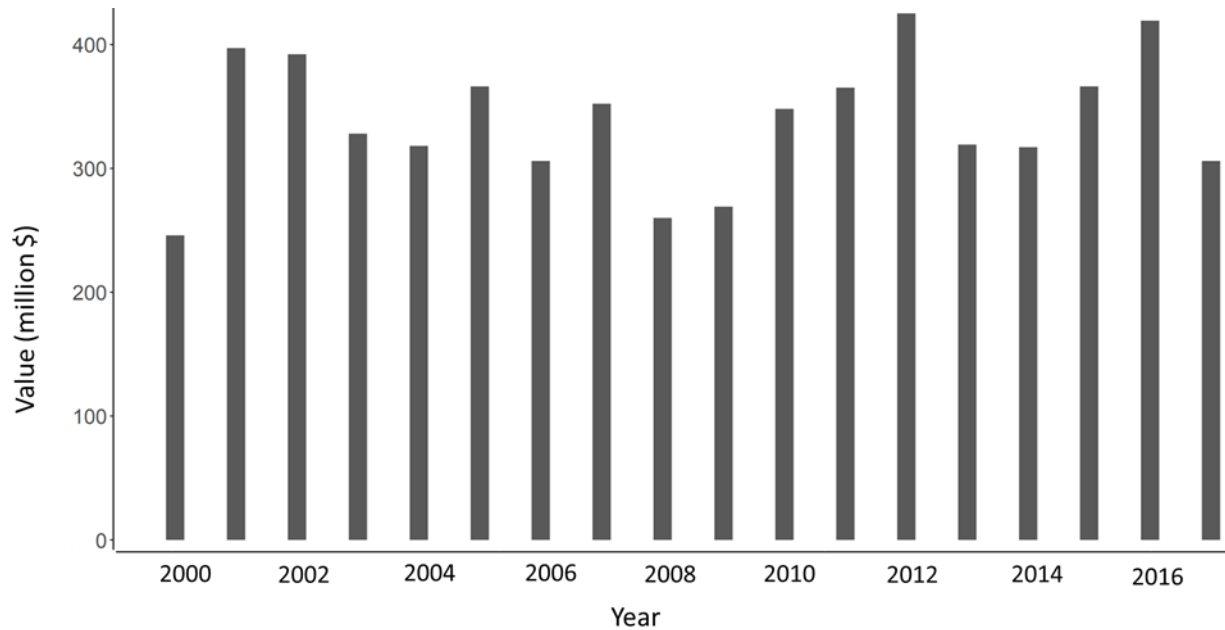
Figure 10: Value of green water in the SNW over the 18-year study period.

4 Discussion

Transpiration is a key process that sustains terrestrial ecosystem functions such as biomass production, and thus helps

to supply a variety of ecosystem services. In the study herein, HGS is used to capture the contributions of subsurface

water storage to transpiration (i.e., productive green water) and quantify its role in sustaining transpiration and

subsequent ecosystem services.

The annual deviations from the long-term means (Fig. 6) show that ET_a and transpiration are supported by the

subsurface and surface storages during droughts. In the drought period from 2001-2002, an interesting situation arises.

In 2001, both ET_a and transpiration exhibit positive values relative to the mean. However, in 2002, despite ET_a being

negative, transpiration remains positive and surpasses the mean value. This deviation can be attributed to the

diminished availability of surface water, leading to reduced evaporation and subsequently lower ET_a. Nevertheless,

transpiration continues to exceed the average due to its reliance on subsurface water availability within the SNW.

Moreover, transpiration primarily relies on biological factors (e.g., land use, NPP), whereas evaporation is

predominantly influenced by meteorological conditions (e.g., air temperature) (Xu et al., 2022). This finding is further

supported by previous studies, which suggest that transpiration dominates ET_a during drought years, while evaporation

takes precedence during wet years (Zhang et al., 2019). To further compare the fluctuations in different storage zones

363   on a common scale, the standard scores (that is, the change in a storage/standard deviation) for each zone are calculated

364   over time (Fig. 11). The standard scores show that ET_a is supported by both surface and subsurface water storages

365   during the drought periods. However, the contribution of subsurface water by volume during drought is much larger

366   than that of surface water, thus highlighting the important role of subsurface water in supporting land surface processes

367   during droughts.
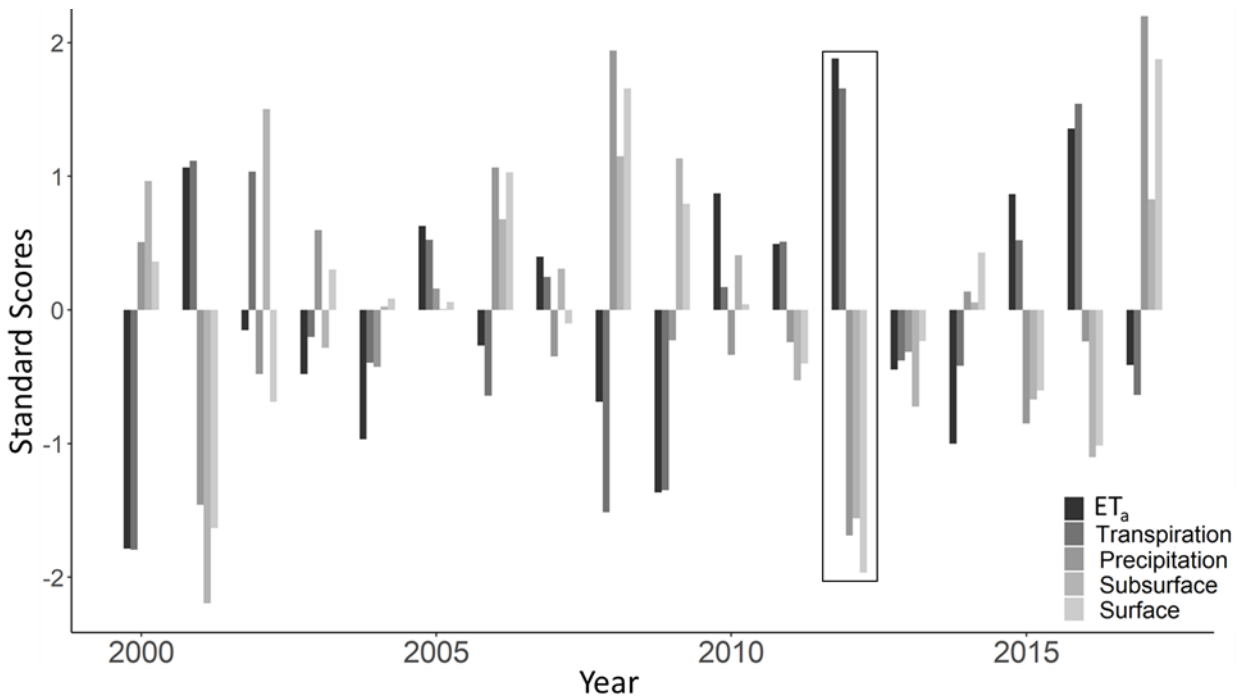
368

369   **Figure 11: Change in standard scores of water storages/hydrological variables over the 18-year study period.**

370   **The scores for the 2012 drought year are bordered.**

371   Comparison of years 2001 and 2012 (both with less precipitation than the 18-year mean) shows that the ET_a was less

372   but outflow was more in year 2001 than in 2012 (Fig. 6(a)). In such case, it is the subsurface water contribution in

373   2001 that maintained the higher surface water flows, which highlights the important role of antecedent conditions in

374   regulating low flow response. The influence of subsurface water on drought behaviour (i.e. years 2001 and 2012) also

375   depends on the timing of precipitation along with other climatic conditions (e.g., temperature, atmospheric moisture

376   demand, etc.) in the corresponding years (Zhao et al., 2022). During drought periods, vegetation and atmospheric

377   moisture demand is often not met, thus resulting in ecosystem stress along with depletion of subsurface and surface

378   water storages (Zhao et al., 2022). Similar to worldwide trends described in Zhao et al. (2022), the transpiration and

379   ET_a rates in the SNW increase during dry periods. Given the complexities involved with linking transpiration with

380 subsurface water storages, full characterization of transpiration influences on ecosystem services during droughts has

381 until now received little attention.

382 The study herein is seminal in quantifying subsurface water ecosystem services values, at the scale of a 3830 km^2

383 watershed, over a period of time that encompasses wide ranging annual climatology. Previous studies (e.g., Loheide,

384 2008; Su et al., 2022) have estimated groundwater contribution to evapotranspiration by linking water table

385 fluctuation with changes in evapotranspiration. However, over large areas, using water table fluctuation can be

386 complicated by other subsurface water sinks, including deeper groundwater recharge and discharge into surface water

387 receptors. With the HGS approach employed herein, the computed subsurface water evaporation and transpiration,

388 and surface water evaporation, in conjunction with the other hydrologic flow processes depicted in Fig. 2, provides a

389 robust characterization of contributions to ET_a.

390 The fluctuations in water storages show that, in general and with respect to longer term mean conditions, subsurface

391 water storage repletes when ET_a is negative and depletes when ET_a is positive. In both the 2001 and 2012 drought

392 years, ET_a is relatively high in comparison to the wet years with high precipitation. ET_a in drought years is primarily

393 supported by the drawdown (by volume) in subsurface water storage below the mean level. In general, fluctuations in

394 subsurface water storage across the 18 years are consistent with changes in precipitation, with above-average

395 precipitation aligned with increases in subsurface water storage and vice-versa. In contrast, increased ET_a leads to a

396 reduction in subsurface storage and vice-versa. Over the 18 year study period, the maximum increase in subsurface

397 water storage occurred in the year 2002, immediately following the 2001 drought which had implications far beyond

398 just the SNW (Wheaton et al., 2008). Even though 2002 was a year with less than average precipitation, the drought

399 impacted subsurface storage conditions led to an antecedent condition across the SNW that was conducive to

400 subsurface water recharge.

401 Regarding the economic valuation of water components, green water mainly benefits people at local scales (by

402 supporting biomass and ecosystem services in the area) whereas the benefits of blue water are seen at larger scales

403 (Falkenmark and Rockström, 2010). Incorporating green-blue water resource consideration at the watershed scale

404 helps with the characterization and quantification of the role water plays in land use and terrestrial ecosystem function.

405 Based on the study herein, fully-integrated groundwater – surface water models, such as HGS, have potential to

406 facilitate better management of watershed scale (approximately 4,000 km^2) water resources for ecosystem services

407 endpoints, and to evaluate the contributions of terrestrial water storages towards green water supply.

408 A water production function was developed using total green water volumes and total values of 13 ecosystem services

409 in the SNW: agricultural services (net benefits from the crops or agricultural products), global climate regulation, air

410 quality, water provision, waste treatment, erosion control, pollination, habitat for biodiversity, natural hazard

411 prevention, pest management, nutrient cycling, landscape aesthetics, and recreational activities. The ecosystem water

412 production function yields a marginal value of \$ 0.26 per m^3 of green water (or transpiration) (Fig. 8). Globally, Lowe

413 et al. (2022) estimated the average marginal product of water specifically for crop production at \$0.083 per m^3.

414 Additional transpiration supplies ecosystem services at a constant rate; however, because the linear line of best fit in

415 Fig. 8 has a positive vertical intercept, the average ecosystem services water productivity decreases with increase in

416 transpiration as the slope of the ray from origin through a point on production function diminishes (Wichelns, 2014).

417 Hence, while water productivity is greatest when the smallest amount of water is used/consumed, it also produces the

418 smallest value of ecosystem services at this point. Between 2000 and 2017, transpiration in the SNW is highest during

419 the driest years in response to drought-associated meteorological conditions such as increase in temperatures (Zhao et

420 al., 2022). However, NPP does not decline during the drought periods, which is consistent with other temperate

421 watershed studies (e.g., Hosen et al., 2019; Sun et al., 2016). Modeling results presented herein show that the drought-

422 induced water stress increases both transpiration and ET_a rates, similar to Zhao et al. (2022) and Diao et al. (2021).

423 During dry years, the increase in transpiration is positively correlated with higher NPP, which in turn relates to lower

424 ecosystem services water productivity (Fig. 9).

425 In the SNW, green water use increases in dry years with less than average precipitation. Accordingly, green water

426 value was highest, at \$424.7 million (in CAD 2022), for the 2012 drought year (Fig. 10). It is important to note that

427 value of the subsurface water contribution is second highest, at 418.63 million, for 2016, which is also a drought year.

428 Hence, the critical role of subsurface water in sustaining ecosystem services is evident during both drought years and

429 more typical years.

430 While the study herein advances the scientific utility of physics-based fully-integrated groundwater–surface water

431 models, it is essential to acknowledge the inherent uncertainty associated with such an analysis, along with factors

432 that could potentially reduce this uncertainty. It is well known that highly parameterized, structurally complex models

433 can have many degrees of freedom, high data requirements, and non-uniqueness challenges (Beven, 2006). However,

434 the parameterization of physics-based models can also be viewed as a strength due to the constraining relationship

435 between physically measurable characteristics and parameter values (Ebel and Loague, 2006). For the SNW, soil and

436 subsurface materials are well characterized and hence the spatial distribution and magnitudes of the associated

437 hydraulic parameters are generally well represented in the HGS model. Incorporating meteorological variability into

438 structurally complex model calibration and performance evaluation can also act to reduce uncertainty (Moeck et al.,

439 2018). Because the SNW simulation extended over an 18-year time frame that included multiple droughts and floods,

440 there is confidence that the model structure and parameterization is suited for a wide spectrum of hydrologic

441 conditions, and that the model can dynamically capture transitions from wet-to-dry and dry-to-wet conditions, which

442 is a critical part of the SNW analysis.

443 It can be posited that physics-based models are best suited for the type of challenge addressed in the work herein

444 because simpler models lack process representation critical within the problem conceptualization (Ebel and Loague,

445 2006). This can be deemed especially true when considering difficulties associated with quantifying large scale

446 evaporation and transpiration (Stoy et al., 2019), and groundwater–surface water interaction (Barthel and Banzhaf,

447 2016). Structurally complex models have been shown to perform better than simple models when simulating

448 evapotranspiration (Ghasemizade et al., 2015) and groundwater recharge (Moeck et al., 2018), and previous work by

449 Hwang et al. (2015) demonstrated the utility of HGS for constraining ET at the watershed scale within the same

450 geographic region as the SNW. Further confidence in the SNW HGS model can be established through comparison

451 with other studies. In terms of overall water balance, results from the study herein compare closely with data compiled

452 as part of regional water management study encompassing the SNW (EOWRMS, 2001). Although the study time

453 frames differ (the EOWRMS (2001) study utilized pre-2000 data), the results are similar, with ETa accounting for

454 approximately 45 % and 62 % of annual precipitation in EOWRMS (2001) and the study herein, respectively. While

455 there is limited previous work investigating the partitioning of ETa into transpiration and evaporation that can be

456 directly compared, it is useful to refer to highly detailed analysis based off Fluxnet data (Pastorello et al., 2020) as

457 reference for transpiration and evaporation partitioning in landcover settings representative of those within the SNW.

458 For example, Xue et al. (2023) reported that transpiration as a percentage of ET ranged from 21-56 % and 39-83 % in

459 Fluxnet cropland and mixed forest settings, respectively, whereas the HGS model predicts an aggregate range of 45-

460 65 % across the SNW watershed, which supports the use of HGS transpiration estimates in subsequent ecosystem

461 services valuation.

462 The methodology employed in this study provides a basis for deploying fully-integrated groundwater – surface water

463 models to assess subsurface water contribution to ecosystem services in other regions. However, it must be noted that

464   the results and values used herein are not necessarily transferable to other sites/watersheds. The marginal product of

465   water is a site-specific entity that will be different for other watersheds because both ecosystem services value and

466   transpiration rate will change in response to factors such as land cover, NPP, climate/weather, hydrogeology, and soil

467   properties. Nevertheless, given the ability of fully-integrated models to quantify the dynamic fluctuation in water

468   storages across different compartments, along with the linkage to terrestrial ecosystem services, the approach can be

469   expected to yield reliable results under similar workflow (modelling of water storages and transpiration rates, and

470   valuation of ecosystem services) for other locations/sites/watersheds.

471   **5 Conclusions**

472   This study characterizes and quantifies the important contribution of subsurface water towards the supply of terrestrial

473   ecosystem services, which, until now has not been comprehensively studied. The prior lack of attention to subsurface

474   water in part relates to the complexities involved with characterizing the dynamic movement of water between

475   subsurface water and surface water storage compartments, and the related supply of green water. In the work herein,

476   focusing on a 3830 km^2 mixed use watershed, the innovative use of a HGS fully-integrated groundwater – surface

477   water model for water ecosystem services valuation is demonstrated, with the endpoint being monetization of the

478   contributions of subsurface water to green water supply over a period of 18 years (2000-2017). Results show that

479   droughts are a major impetus for increased green water use. The maximum annual green water value was $424.7

480   million (CAD 2022) during the 2012 drought year, while the 18-year average was $338.83 million. Similarly, in other

481   dry years (i.e., 2001-2002 and 2016), there was a discernible rise in the green water use. Conversely, the results show

482   a notable decrease in the green water use during years characterized by higher precipitation, as exemplified in the year

483   2000 where green water provided $245.9 million in ecosystem services value. Hence, the study emphasizes the key

484   role of subsurface water in supplying green water and sustaining ecosystem services during critical periods when the

485   watershed is under meteorological drought. The methodology developed herein is extensible to other watersheds and

486   provides the ability to improve characterization of water ecosystem services and to better value and manage subsurface

487   water resources under current and future climate conditions.

Author contribution

Tariq Aziz contributed to concept development, methodology, formal analysis, investigation, and writing the original draft.

Steven K. Frey contributed to concept development, methodology, data curation, HGS modeling, project administration, and reviewing and editing the manuscript.

David R. Lapen contributed to methodology development, reviewing and editing the manuscript, and project administration.

Susan Preston contributed to methodology development, reviewing and editing the manuscript, and project administration.

Hazen A. J. Russell contributed to hydrogeologic characterization, and with reviewing and editing the manuscript.

Omar Khader contributed to data curation, HGS model development, and formal analysis.

Andre R. Erler contributed to data curation and reviewing the manuscript.

Edward A. Sudicky contributed to project administration and reviewing the manuscript.

Declaration of interest

The authors declare that they have no known competing financial interests or personal relationships that could have appeared to influence the work reported in this paper.

References

Agriculture and Agri-Food Canada: Annual Space-Based Crop Inventory for Canada, 2017, Agroclimate, Geomatics and Earth Observation Division, Science and Technology Branch, 2017.

Allen, R. G., Pereira, L. S., Raes, D., and Smith, M.: Crop evapotranspiration guidelines for computing crop requirements, 1998. Available at: https://www.fao.org/3/X0490E/x0490e00.htm

An, S. and Verhoeven, J. T. A.: Wetlands: Ecosystem services, restoration and wise use, Springer, 325 pp., https://doi.org/10.1007/978-3-030-14861-4, 2019.

Aquanty: HydroGeoSphere: A three-dimensional numerical model describing fully-integrated subsurface and surface flow and solute transport, Waterloo, 2021.

Arnold, J. G., Srinivasan, R., Muttiah, R. S., and Williams, J. R.: Large area hydrologic modeling and assessment part I: Model development, J. Am. Water Resour. Assoc., 34, 73–89, https://doi.org/10.1111/j.1752-1688.1998.tb05961.x, 1998.

Aziz, T.: Changes in land use and ecosystem services values in Pakistan, 1950–2050, Environ. Dev., 35, 13, https://doi.org/10.1016/j.envdev.2020.100576, 2021.

Barthel, R. and Banzhaf, S.: Groundwater and Surface Water Interaction at the Regional-scale – A Review with Focus on Regional Integrated Models, Water Resour. Manag., 30, 1–32, https://doi.org/10.1007/s11269-015-1163-z, 2016.

Berg, S. J. and Sudicky, E. A.: Toward Large-Scale Integrated Surface and Subsurface Modeling, Groundwater, 57, 1–2, https://doi.org/10.1111/gwat.12844, 2019.

522 Beven, K.: A manifesto for the equifinality thesis, J. Hydrol., 320, 18–36,
523 https://doi.org/10.1016/j.jhydrol.2005.07.007, 2006.

524 Bolte, J.: Envision integrated modeling platform, 94 pp., 2022.

525 Booth, E. G., Zipper, S. C., Loheide, S. P., and Kucharik, C. J.: Is groundwater recharge always serving us well?
526 Water supply provisioning, crop production, and flood attenuation in conflict in Wisconsin, USA, Ecosyst. Serv., 21,
527 153–165, 2016.

528 Brunner, P. and Simmons, C. T.: HydroGeoSphere: A Fully Integrated, Physically Based Hydrological Model, Ground
529 Water, 50, 170–176, https://doi.org/10.1111/j.1745-6584.2011.00882.x, 2012.

530 Casagrande, E., Recanati, F., Cristina, M., Bevacqua, D., and Meli, P.: Water balance partitioning for ecosystem
531 service assessment. A case study in the Amazon, Ecol. Indic., 121, https://doi.org/10.1016/j.ecolind.2020.107155,
532 2021.

533 Chen, X. and Hu, Q.: Groundwater influences on soil moisture and surface evaporation, J. Hydrol., 297, 285–300,
534 https://doi.org/10.1016/j.jhydrol.2004.04.019, 2004.

535 Clark, M. P., Fan, Y., Lawrence, D. M., Adam, J. C., Bolster, D., Gochis, D. J., Hooper, R. P., Kumar, M., Leung, L.
536 R., Mackay, D. S., and Maxwell, R. M.: Hydrological partitioning in the critical zone: Recent advances and
537 opportunities for developing transferable understanding of water cycle dynamics, Water Resour. Res., 1–28,
538 https://doi.org/10.1002/2015WR017096.Received, 2015.

539 Condon, L. E., Atchley, A. L., and Maxwell, R. M.: Evapotranspiration depletes groundwater under warming over the
540 contiguous United States, Nat. Commun., 11, https://doi.org/10.1038/s41467-020-14688-0, 2020.

541 Costanza, R., D'Arge, R., De Groot, R., Farber, S., Grasso, M., Hannon, B., Limburg, K., Naeem, S., O'Neill, R. V.,
542 Paruelo, J., Raskin, R. G., Sutton, P., and Van Den Belt, M.: The value of ecosystem services: Putting the issues in
543 perspective, Ecol. Econ., 25, 67–72, https://doi.org/10.1016/S0921-8009(98)00019-6, 1998.

544 Decsi, B., Ács, T., Jolánkai, Z., Kardos, M. K., Koncsos, L., Vári, Á., and Kozma, Z.: From simple to complex –
545 Comparing four modelling tools for quantifying hydrologic ecosystem services, Ecol. Indic., 141,
546 https://doi.org/10.1016/j.ecolind.2022.109143, 2022.

547 Dennedy-Frank, P. J., Muenich, R. L., Chaubey, I., and Ziv, G.: Comparing two tools for ecosystem service
548 assessments regarding water resources decisions, J. Environ. Manage., 177, 331–340,
549 https://doi.org/10.1016/j.jenvman.2016.03.012, 2016.

550 Diao, H., Wang, A., Yang, H., Yuan, F., Guan, D., and Wu, J.: Responses of evapotranspiration to droughts across
551 global forests: A systematic assessment, Can. J. For. Res., 51, 1–9, https://doi.org/10.1139/cjfr-2019-0436, 2021.

552 Ebel, B. A. and Loague, K.: Physics-based hydrologic-response simulation: Seeing through the fog of equifinality,
553 Hydrol. Process., 20, 2887–2900, https://doi.org/10.1002/hyp.6388, 2006.

554 Endsley, K. A., Zhao, M., Kimball, J., and Deva, S.: Continuity of global MODIS terrestrial primary productivity
555 estimates in the VIIRS era using model-data fusion, J. Geophys. Res. Biogeosciences,
556 https://doi.org/10.22541/essoar.167768101.16068273/v1, 2023.

557 EOWRMS: Eastern Ontario water resources management study (final report), Ottawa, Ontario, 5–24 pp., 2001.

558 Erler, A. R., Frey, S. K., Khader, O., d'Orgeville, M., Park, Y. J., Hwang, H. T., Lapen, D. R., Richard Peltier, W.,

and Sudicky, E. A.: Simulating Climate Change Impacts on Surface Water Resources Within a Lake-Affected Region Using Regional Climate Projections, Water Resour. Res., 55, 130–155, https://doi.org/10.1029/2018WR024381, 2019.

Falkenmark, M. and Rockström, J.: Building Water Resilience in the Face of Global Change: From a Blue-Only to a Green-Blue Water Approach to Land-Water Management, J. Water Resour. Plan. Manag., 136, 606–610, https://doi.org/10.1061/(asce)wr.1943-5452.0000118, 2010.

Foster, S. S. D. and Chilton, P. J.: Groundwater: The processes and global significance of aquifer degradation, Philos. Trans. R. Soc. B Biol. Sci., 358, 1957–1972, https://doi.org/10.1098/rstb.2003.1380, 2003.

Frey, S. K., Miller, K., Khader, O., Taylor, A., Morrison, D., Xu, X., Berg, S. J., Sudicky, E. A., and Lapen, D. R.: Evaluating landscape influences on hydrologic behavior with a fully- integrated groundwater – surface water model, J. Hydrol., 602, 1–8, 2021.

Ghasemizade, M., Moeck, C., and Schirmer, M.: The effect of model complexity in simulating unsaturated zone flow processes on recharge estimation at varying time scales, J. Hydrol., 529, 1173–1184, https://doi.org/10.1016/j.jhydrol.2015.09.027, 2015.

Griebler, C. and Avramov, M.: Groundwater ecosystem services: A review, Freshw. Sci., 34, 355–367, https://doi.org/10.1086/679903, 2015.

Hogg, E. H.: Temporal scaling of moisture and the forest-grassland boundary in western Canada, Agric. For. Meteorol., 84, 115–122, https://doi.org/10.1016/S0168-1923(96)02380-5, 1997.

Honeck, E., Gallagher, L., von Arx, B., Lehmann, A., Wyler, N., Villarrubia, O., Guinaudeau, B., and Schlaepfer, M. A.: Integrating ecosystem services into policymaking – A case study on the use of boundary organizations, Ecosyst. Serv., 49, https://doi.org/10.1016/j.ecoser.2021.101286, 2021.

Hosen, J. D., Aho, K. S., Appling, A. P., Creech, E. C., Fair, J. H., Hall, R. O., Kyzivat, E. D., Lowenthal, R. S., Matt, S., Morrison, J., Saiers, J. E., Shanley, J. B., Weber, L. C., Yoon, B., and Raymond, P. A.: Enhancement of primary production during drought in a temperate watershed is greater in larger rivers than headwater streams, Limnol. Oceanogr., 64, 1458–1472, https://doi.org/10.1002/lno.11127, 2019.

Hwang, H. T., Park, Y. J., Frey, S. K., Berg, S. J., and Sudicky, E. A.: A simple iterative method for estimating evapotranspiration with integrated surface/subsurface flow models, J. Hydrol., 531, 949–959, https://doi.org/10.1016/j.jhydrol.2015.10.003, 2015.

Jin, Z., Liang, W., Yang, Y., Zhang, W., Yan, J., Chen, X., Li, S., and Mo, X.: Separating Vegetation Greening and Climate Change Controls on Evapotranspiration trend over the Loess Plateau, Sci. Rep., 7, 1–15, https://doi.org/10.1038/s41598-017-08477-x, 2017.

Kollet, S., Mauro, S., M., M. R., Paniconi, C., Putti, M., Bertoldi, G., Coon, E. T., Cordano, E., Endrizzi, S., Kikinzon, E., Mouche, E., M€ugler, C., Park, Y.-J., Refsgaard, J. C., Stisen, S., and Sudicky, E.: The integrated hydrologic model intercomparison project, IH-MIP2: A second set of benchmark results to diagnose integrated hydrology and feedbacks, Water Resour. Res., 867–890, https://doi.org/10.1002/2016WR019191.Received, 2016.

Kornelsen, K. C. and Coulibaly, P.: Synthesis review on groundwater discharge to surface water in the Great Lakes Basin, J. Great Lakes Res., 40, 247–256, https://doi.org/10.1016/j.jglr.2014.03.006, 2014.

596 L'Ecuyer-Sauvageau, C., Dupras, J., He, J., Auclair, J., Kermagoret, C., and Poder, T. G.: The economic value of
597 Canada's National Capital Green Network, PLoS One, 16, 1–29, https://doi.org/10.1371/journal.pone.0245045, 2021.
598 Li, Q., Qi, J., Xing, Z., Li, S., Jiang, Y., Danielescu, S., Zhu, H., Wei, X., and Meng, F. R.: An approach for assessing
599 impact of land use and biophysical conditions across landscape on recharge rate and nitrogen loading of groundwater,
600 Agric. Ecosyst. Environ., 196, 114–124, https://doi.org/10.1016/j.agee.2014.06.028, 2014.
601 Liang, X., Lettenmaier, D. P., Wood, E. F., and Burges, S. J.: A simple hydrologically based model of land surface
602 water and energy fluxes for general circulation models, J. Geophys. Res., 99, https://doi.org/10.1029/94jd00483, 1994.
603 Liu, Y. and El-Kassaby, Y. A.: Evapotranspiration and favorable growing degree-days are key to tree height growth
604 and ecosystem functioning: Meta-Analyses of Pacific Northwest historical data, 1st Annu. IEEE Conf. Control
605 Technol. Appl. CCTA 2017, 2017-Janua, 7–12, https://doi.org/10.1038/s41598-018-26681-1, 2017.
606 Liu, Y., Zhou, R., Wen, Z., Khalifa, M., Zheng, C., Ren, H., Zhang, Z., and Wang, Z.: Assessing the impacts of
607 drought on net primary productivity of global land biomes in different climate zones, Ecol. Indic., 130, 108146,
608 https://doi.org/10.1016/j.ecolind.2021.108146, 2021.
609 Logan, C., Cummings, D. I., Pullan, S., Pugin, A., Russell, H. A. J., and Sharpe, D. R.: Hydrostratigraphic model of
610 the South Nation watershed region, south-eastern Ontario, Geological Survey of Canada, 17 pp.,
611 https://doi.org/https://doi.org/10.4095/248203, 2009.
612 Loheide, S. P.: A method for estimating subdaily evapotranspiration of shallow groundwater using diurnal water table
613 fluctuations, Ecohydrology, 1, 59–66, 2008.
614 Lowe, B. H., Zimmer, Y., and Oglethorpe, D. R.: Estimating the economic value of green water as an approach to
615 foster the virtual green-water trade, Ecol. Indic., 136, 108632, https://doi.org/10.1016/j.ecolind.2022.108632, 2022.
616 Mammola, S., Cardoso, P., Culver, D. C., Deharveng, L., Ferreira, R. L., Fišer, C., Galassi, D. M. P., Griebler, C.,
617 Halse, S., Humphreys, W. F., Isaia, M., Malard, F., Martinez, A., Moldovan, O. T., Niemiller, M. L., Pavlek, M.,
618 Reboleira, A. S. P. S., Souza-Silva, M., Teeling, E. C., Wynne, J. J., and Zagmajster, M.: Scientists' warning on the
619 conservation of subterranean ecosystems, Bioscience, 69, 641–650, https://doi.org/10.1093/biosci/biz064, 2019.
620 Maxwell, R. M., Putti, M., Meyerhoff, S., Delfs, J.-O., Ferguson, I. M., Ivanov, V., Jongho Kim, O. K., Stefan J.
621 Kollet, M. K., Lopez, S., Jie Niu, Claudio Paniconi, Y.-J. P., Mantha S. Phanikumar, C. S., Sudicky, E. A., and Sulis,
622 M.: Surface-subsurface model intercomparison: A first set of benchmark results to diagnose integrated hydrology and
623 feedbacks, Water Resour. Res., 1531–1549, https://doi.org/10.1002/2013WR013725.Received, 2014.
624 McKenney, D. W., Hutchiinson, M. F., Papadopol, P., Lawrence, K., Pedlar, J., Campbell, K., Milewska, E.,
625 Hopkinson, R. F., Price, D., and Owen, T.: Customized spatial climate models for North America, Bull. Am. Meteorol.
626 Soc., 92, 1611–1622, https://doi.org/10.1175/2011BAMS3132.1, 2011.
627 Mercado-bettín, D., Salazar, J. F., and Villegas, J. C.: Long-term water balance partitioning explained by physical and
628 ecological characteristics in world river basins, Ecohydrology, 12, 1–13,
629 https://doi.org/https://doi.org/10.1002/eco.2072, 2019.
630 Millenium Ecosystem Assessment (MEA): Ecosystems and Human Well-Being: Synthesis, Island Press, 285 pp.,
631 https://doi.org/10.1057/9780230625600, 2005.
632 Moeck, C., von Freyberg, J., and Schirmer, M.: Groundwater recharge predictions in contrasted climate: The effect of

model complexity and calibration period on recharge rates, Environ. Model. Softw., 103, 74–89, https://doi.org/10.1016/j.envsoft.2018.02.005, 2018.

Moriasi, D. N., Arnold, J. G., Van Liew, M. W., Bingner, R. L., Harmel, R. D., and Veith, T. L.: Model evaluation guidelines for systematic quantification of accuracy in watershed simulations, Trans. ASABE, 50, 885–900, https://doi.org/10.13031/2013.23153, 2007.

Mulligan, M.: User guide for the Co$ting Nature Policy Support System v.2., https://goo.gl/Grpbnb, 2015.

Muñoz-Sabater, J., Dutra, E., Agustí-Panareda, A., Albergel, C., Arduini, G., Balsamo, G., Boussetta, S., Choulga, M., Harrigan, S., Hersbach, H., Martens, B., Miralles, D. G., Piles, M., Rodríguez-Fernández, N. J., Zsoter, E., Buontempo, C., and Thépaut, J. N.: ERA5-Land: A state-of-the-art global reanalysis dataset for land applications, Earth Syst. Sci. Data, 13, 4349–4383, https://doi.org/10.5194/essd-13-4349-2021, 2021.

MYD15A2H MODIS/Aqua Leaf Area Index/FPAR 8-Day L4 Global 500m SIN Grid. NASA LP DAAC:

Natural Capital Project: InVEST User Guide 3.12.0, 1–7 pp., 2022.

Neff, B. P., Day, S. M., Piggott, A. R., and Fuller, L. M.: Base flow in the Great Lakes basin, U.S. Geol. Surv. Sci. Investig. Rep., 32, 2005.

Ochoa, V. and Urbina-Cardona, N.: Tools for spatially modeling ecosystem services: Publication trends, conceptual reflections and future challenges, Ecosyst. Serv., 26, 155–169, https://doi.org/10.1016/j.ecoser.2017.06.011, 2017.

Ontario Geological Survey: Surficial Geology of Southern Ontario, Miscellaneous Release--Data 128-REV. Ontario Geological Survey., 1–7 pp., 2010.

Ontario Integrated Hydrology Data: https://geohub.lio.gov.on.ca/maps/mnrf::ontario-integrated-hydrology-oih-data/about.

Pastorello, G., Trotta, C., Canfora, E., Chu, H., Christianson, D., Cheah, Y. W., Poindexter, C., Chen, J., Elbashandy, A., Humphrey, M., Isaac, P., Polidori, D., Ribeca, A., van Ingen, C., Zhang, L., Amiro, B., Ammann, C., Arain, M. A., Ardö, J., Arkebauer, T., Arndt, S. K., Arriga, N., Aubinet, M., Aurela, M., Baldocchi, D., Barr, A., Beamesderfer, E., Marchesini, L. B., Bergeron, O., Beringer, J., Bernhofer, C., Berveiller, D., Billesbach, D., Black, T. A., Blanken, P. D., Bohrer, G., Boike, J., Bolstad, P. V., Bonal, D., Bonnefond, J. M., Bowling, D. R., Bracho, R., Brodeur, J., Brümmer, C., Buchmann, N., Burban, B., Burns, S. P., Buysse, P., Cale, P., Cavagna, M., Cellier, P., Chen, S., Chini, I., Christensen, T. R., Cleverly, J., Collalti, A., Consalvo, C., Cook, B. D., Cook, D., Coursolle, C., Cremonese, E., Curtis, P. S., D'Andrea, E., da Rocha, H., Dai, X., Davis, K. J., De Cinti, B., de Grandcourt, A., De Ligne, A., De Oliveira, R. C., Delpierre, N., Desai, A. R., Di Bella, C. M., di Tommasi, P., Dolman, H., Domingo, F., Dong, G., Dore, S., Duce, P., Dufrêne, E., Dunn, A., Dušek, J., Eamus, D., Eichelmann, U., ElKhidir, H. A. M., Eugster, W., Ewenz, C. M., Ewers, B., Famulari, D., Fares, S., Feigenwinter, I., Feitz, A., Fensholt, R., Filippa, G., Fischer, M., Frank, J., Galvagno, M., Gharun, M., Gianelle, D., et al.: The FLUXNET2015 dataset and the ONEFlux processing pipeline for eddy covariance data, Sci. Data, 7, 1–27, https://doi.org/10.1038/s41597-020-0534-3, 2020.

Qiu, J., Zipper, S. C., Motew, M., Booth, E. G., Kucharik, C. J., and Loheide, S. P.: Nonlinear groundwater influence on biophysical indicators of ecosystem services, Nat. Sustain., 2, 475–483, https://doi.org/10.1038/s41893-019-0278-2, 2019.

Richardson, M. and Kumar, P.: Critical Zone services as environmental assessment criteria in intensively managed

670   landscapes, Earth's Futur., 5, 617–632, https://doi.org/10.1002/2016EF000517, 2017.

671   Schaap, M. G., Leij, F. J., and Van Genuchten, M. T.: Rosetta: A computer program for estimating soil hydraulic

672   parameters with hierarchical pedotransfer functions, J. Hydrol., 251, 163–176, https://doi.org/10.1016/S0022-

673   1694(01)00466-8, 2001.

674   Schyns, J. F., Hoekstra, A. Y., Booij, M. J., Hogeboom, R. J., and Mekonnen, M. M.: Limits to the world's green

675   water resources for food, feed, fiber, timber, and bioenergy, Proc. Natl. Acad. Sci. U. S. A., 116, 4893–4898,

676   https://doi.org/10.1073/pnas.1817380116, 2019.

677   Siebert, S., Burke, J., Faures, J. M., Frenken, K., Hoogeveen, J., Döll, P., and Portmann, F. T.: Groundwater use for

678   irrigation - A global inventory, Hydrol. Earth Syst. Sci., 14, 1863–1880, https://doi.org/10.5194/hess-14-1863-2010,

679   2010.

680   SLC: Soil Landscapes of Canada Version 3.2, 2007–2008 pp., 2010.

681   Stoy, P. C., El-Madany, T. S., Fisher, J. B., Gentine, P., Gerken, T., Good, S. P., Klosterhalfen, A., Liu, S., Miralles,

682   D. G., Perez-Priego, O., Rigden, A. J., Skaggs, T. H., Wohlfahrt, G., Anderson, R. G., Coenders-Gerrits, A. M. J.,

683   Jung, M., Maes, W. H., Mammarella, I., Mauder, M., Migliavacca, M., Nelson, J. A., Poyatos, R., Reichstein, M.,

684   Scott, R. L., and Wolf, S.: Reviews and syntheses: Turning the challenges of partitioning ecosystem evaporation and

685   transpiration into opportunities, Biogeosciences, 16, 3747–3775, https://doi.org/10.5194/bg-16-3747-2019, 2019.

686   Su, Y., Feng, Q., Zhu, G., Wang, Y., and Zhang, Q.: A New Method of Estimating Groundwater Evapotranspiration

687   at   Sub-Daily   Scale   Using   Water   Table   Fluctuations,   Water   (Switzerland),   14,   1–14,

688   https://doi.org/10.3390/w14060876, 2022.

689   Sun, B., Zhao, H., and Wang, X.: Effects of drought on net primary productivity: Roles of temperature, drought

690   intensity, and duration, Chinese Geogr. Sci., 26, 270–282, https://doi.org/10.1007/s11769-016-0804-3, 2016.

691   Sun, G., Hallema, D., and Asbjornsen, H.: Ecohydrological processes and ecosystem services in the Anthropocene: a

692   review, Ecol. Process., 6, https://doi.org/10.1186/s13717-017-0104-6, 2017.

693   Tan, S., Wang, H., Prentice, I. C., and Yang, K.: Land-surface evapotranspiration derived from a first-principles

694   primary production model, Environ. Res. Lett., 16, https://doi.org/10.1088/1748-9326/ac29eb, 2021.

695   Taylor, R. G., Scanlon, B., Döll, P., Rodell, M., Van Beek, R., Wada, Y., Longuevergne, L., Leblanc, M., Famiglietti,

696   J. S., Edmunds, M., Konikow, L., Green, T. R., Chen, J., Taniguchi, M., Bierkens, M. F. P., Macdonald, A., Fan, Y.,

697   Maxwell, R. M., Yechieli, Y., Gurdak, J. J., Allen, D. M., Shamsudduha, M., Hiscock, K., Yeh, P. J. F., Holman, I.,

698   and   Treidel,   H.:   Ground   water   and   climate   change,   Nat.   Clim.   Chang.,   3,   322–329,

699   https://doi.org/10.1038/nclimate1744, 2013.

700   Vigerstol, K. L. and Aukema, J. E.: A comparison of tools for modeling freshwater ecosystem services, J. Environ.

701   Manage., 92, 2403–2409, https://doi.org/10.1016/j.jenvman.2011.06.040, 2011.

702   Villa, F., Bagstad, K., and Balbi, S.: ARIES: Artificial Intelligence for Environment & Sustainability, 2021.

703   Wheaton, E., Kulshreshtha, S., Wittrock, V., and Koshida, G.: Dry times: Hard lessons from the Canadian drought of

704   2001 and 2002, Can. Geogr., 52, 241–262, https://doi.org/10.1111/j.1541-0064.2008.00211.x, 2008.

705   Wichelns, D.: Do estimates of water productivity enhance understanding of farm-level water management?, Water

706   (Switzerland), 6, 778–795, https://doi.org/10.3390/w6040778, 2014.

Xu, C., Li, Y., Hu, J., Yang, X., Sheng, S., and Liu, M.: Evaluating the difference between the normalized difference vegetation index and net primary productivity as the indicators of vegetation vigor assessment at landscape scale, Environ. Monit. Assess., 184, 1275–1286, https://doi.org/10.1007/s10661-011-2039-1, 2012.

Xu, M., An, T., Zheng, Z., Zhang, T., Zhang, Y., and Yu, G.: Variability in evapotranspiration shifts from meteorological to biological control under wet versus drought conditions in an alpine meadow, J. Plant Ecol., 15, 921–932, https://doi.org/10.1093/jpe/rtac033, 2022.

Xu, S., Frey, S. K., Erler, A. R., Khader, O., Berg, S. J., Hwang, H. T., Callaghan, M. V., Davison, J. H., and Sudicky, E. A.: Investigating groundwater-lake interactions in the Laurentian Great Lakes with a fully-integrated surface water-groundwater model, J. Hydrol., 594, 125911, https://doi.org/10.1016/j.jhydrol.2020.125911, 2021.

Xu, Y. and Xiao, F.: Assessing Changes in the Value of Forest Ecosystem Services in Response to Climate Change in China, Sustain., 14, https://doi.org/10.3390/su14084773, 2022.

Xue, K., Song, L., Xu, Y., Liu, S., Zhao, G., Tao, S., Magliulo, E., Manco, A., Liddell, M., Wohlfahrt, G., Varlagin, A., Montagnani, L., Woodgate, W., Loubet, B., and Zhao, L.: Estimating ecosystem evaporation and transpiration using a soil moisture coupled two-source energy balance model across FLUXNET sites, Agric. For. Meteorol., 337, 1–7, https://doi.org/10.1016/j.agrformet.2023.109513, 2023.

Yang, H., Luo, P., Wang, J., Mou, C., Mo, L., Wang, Z., Fu, Y., Lin, H., Yang, Y., and Bhatta, L. D.: Ecosystem evapotranspiration as a response to climate and vegetation coverage changes in Northwest Yunnan, China, PLoS One, 10, 1–17, https://doi.org/10.1371/journal.pone.0134795, 2015.

Yang, X. and Liu, J.: Assessment and valuation of groundwater ecosystem services: A case study of Handan City, China, Water (Switzerland), 12, https://doi.org/10.3390/w12051455, 2020.

Yu, S., Miao, C., Song, H., Huang, Y., and Chen, W.: Efficiency of nitrogen and phosphorus removal by six macrophytes from eutrophic water Efficiency of nitrogen and phosphorus removal by six macrophytes from eutrophic water, Int. J. Phytoremediation, 21, 643–651, https://doi.org/10.1080/15226514.2018.1556582, 2019.

Zhang, T., Xu, M., Zhang, Y., Zhao, T., An, T., Li, Y., Sun, Y., Chen, N., Zhao, T., Zhu, J., and Yu, G.: Grazing-induced increases in soil moisture maintain higher productivity during droughts in alpine meadows on the Tibetan Plateau, Agric. For. Meteorol., 269–270, 249–256, https://doi.org/10.1016/j.agrformet.2019.02.022, 2019.

Zhao, M., Aa, G., Liu, Y., and Konings, A.: Evapotranspiration frequently increases during droughts, Nat. Clim. Chang., 6904, 2022.

Zisopoulou, K., Zisopoulos, D., and Panagoulia, D.: Water Economics: An In-Depth Analysis of the Connection of Blue Water with Some Primary Level Aspects of Economic Theory I, Water (Switzerland), 14, https://doi.org/10.3390/w14010103, 2022.

Appendix

The annual outputs (ET_a, surface water, subsurface water, precipitation and outflow) from the HGS model are given in Table 1A.

Table A1: HGS outputs from the SNW simulation

Year	ET$_a$ (m³)	Surface water (m³)	Subsurface water (m³)	Precipitation (m³)	Outflow (m³)	Surface evaporation (m³)	Subsurface evaporation (m³)	Subsurface transpiration (m³)
2000	2,085,534,445	69,424,628	222,709,069,460	4,199,527,096	76,327,719	75,020,473	184,374,990	945,999,818
2001	2,477,004,097	54,513,422	222,240,461,950	3,003,497,233	32,382,847	49,049,150	193,684,126	1,525,263,969
2002	2,309,984,877	61,588,887	222,788,771,412	3,598,706,939	50,743,315	49,496,381	137,246,184	150,943,1,700
2003	2,264,696,091	68,998,342	222,524,086,305	4,253,877,105	64,623,628	63,041,934	155,345,628	1,263,073,935
2004	2,197,974,479	67,358,376	222,569,571,666	3,631,932,688	47,291,949	56,472,059	186,217,551	1,224,545,264
2005	2,416,958,064	67,153,617	222,566,818,892	3,988,298,138	48,434,304	62,293,999	203,745,742	1407,718,083
2006	2,293,950,204	74,422,486	222,666,754,361	4,538,849,536	77,813,027	73,310,604	176,406,194	1,175,390,417
2007	2,385,260,383	65,967,543	222,611,557,149	3,679,748,277	47,306,909	55,442,956	193,054,015	1,352,247,667
2008	2,236,139,918	79,130,070	222,736,726,608	5,070,858,236	75,918,796	63,243,999	153,505,172	1,001,912,242
2009	2,142,956,266	72,673,133	222,733,824,127	3,753,041,839	73,573,865	74,320,182	175,808,767	1,034,718,786
2010	2,450,480,102	67,043,193	222,626,541,197	3,686,832,140	67,076,288	78,166,506	204,928,373	1,337,194,629
2011	2,398,275,129	63,710,702	222,487,837,813	3,743,641,761	47,912,738	56,432,877	170,459,783	1,404,943,119

2012	2,589,094,745	52,013,667	222,334,569,769	2,864,258,811	26,234,849	58,974,276	223,348,145	1,633,465,101
2013	2,269,228,484	64,978,113	222,458,625,710	3,700,833,331	54,270,475	67,961,698	205,253,614	1,227,712,022
2014	2,193,041,030	69,944,514	222,574,462,508	3,974,971,693	44,803,342	67,115,318	170,740,982	1,220,179,455
2015	2,449,702,370	62,201,787	222,466,595,816	3,374,434,139	14,781,188	64,640,268	227,937,634	1,407,052,424
2016	2,516,780,613	59,120,794	222,402,665,868	3,747,442909	40,697,558	53,448,526	220,313,313	1,610,087,162
2017	2,273,903,311	80,775,412	222,688,809,435	5,228,987,865	63,739,372	77,841,432	192,369,477	1,176,497,385

745

The SNW has approximately 110 m of vertical relief from its highest point in the southwest corner to its outlet at the Ottawa River at its northern edge (Fig. 1A).
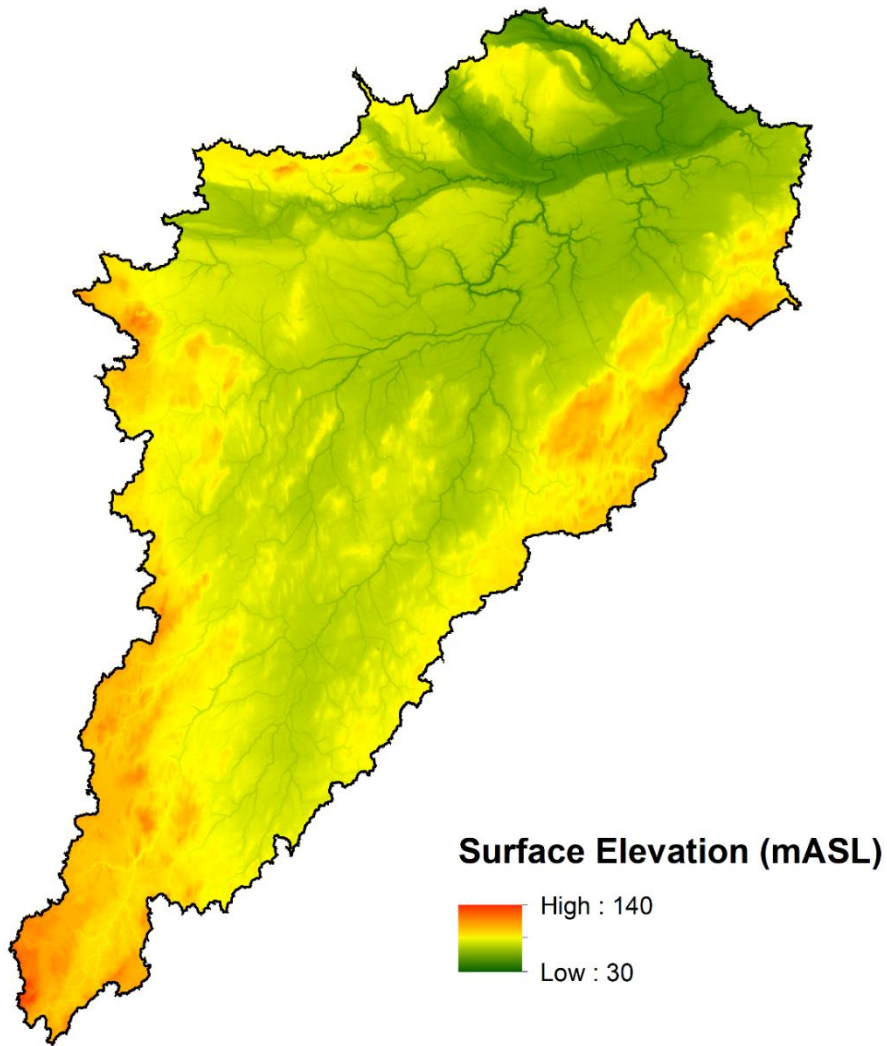
Figure 1A: Land surface elevation of the SNW (Ontario Integrated Hydrology Data).
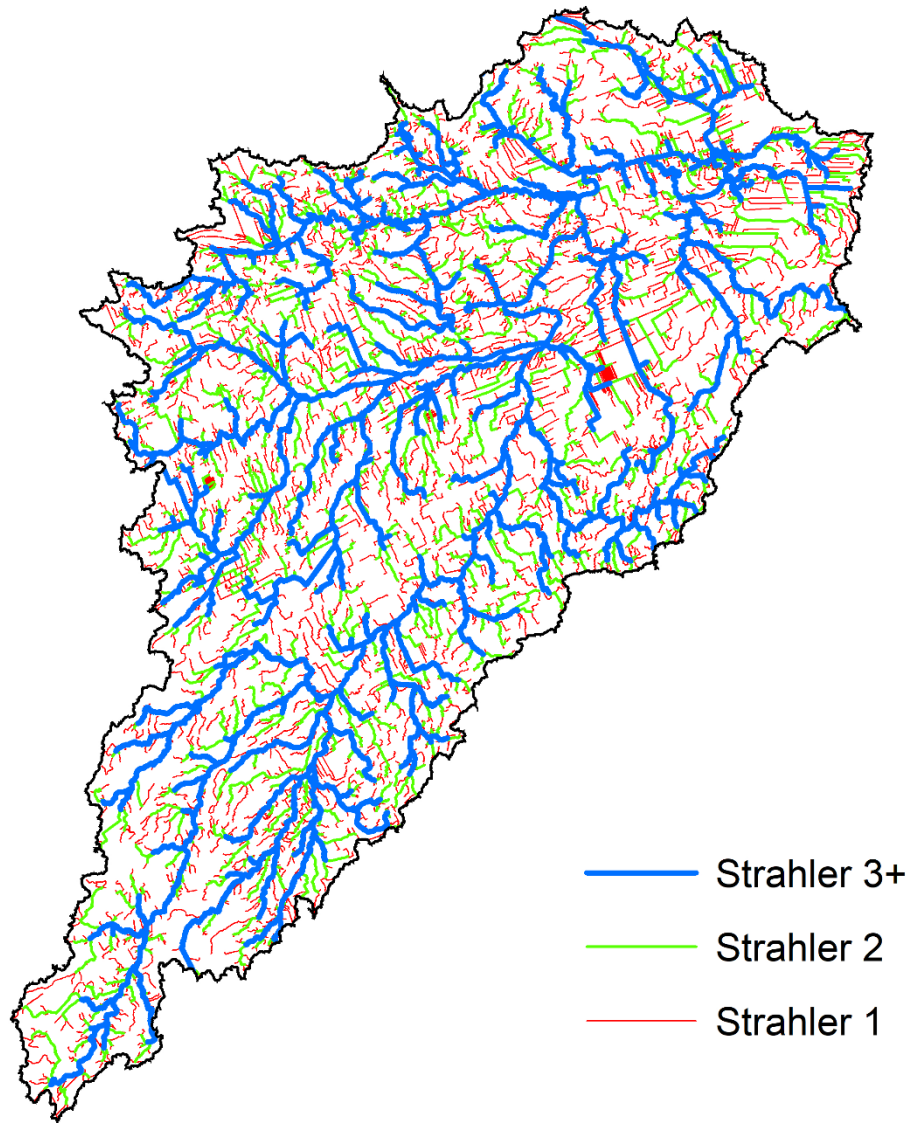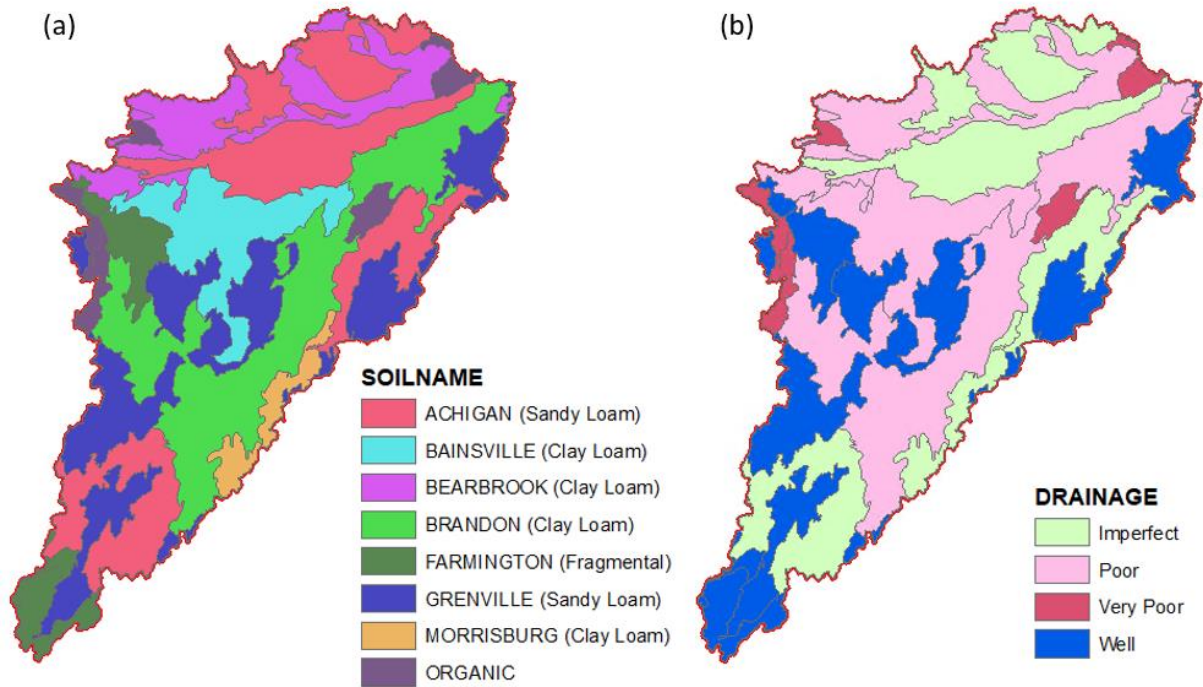
750

Figure 2A. Stream network distribution across the South Nation watershed, consisting of 1606 km of Strahler 3+ streams, 1548 km of Strahler 2 streams, and 3335 km of Strahler 1 streams (Ontario Ministry of Natural Resources and Forestry 2013).

755

Figure 3A. (a) Soil distribution, and (b) soil drainage status across the South Nation watershed (SLC, 2010) .
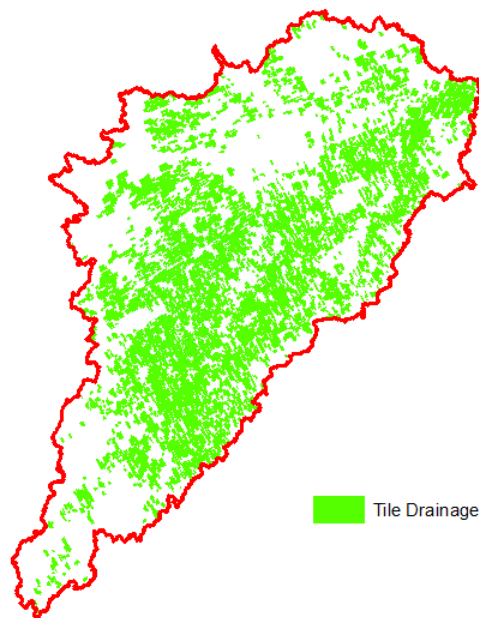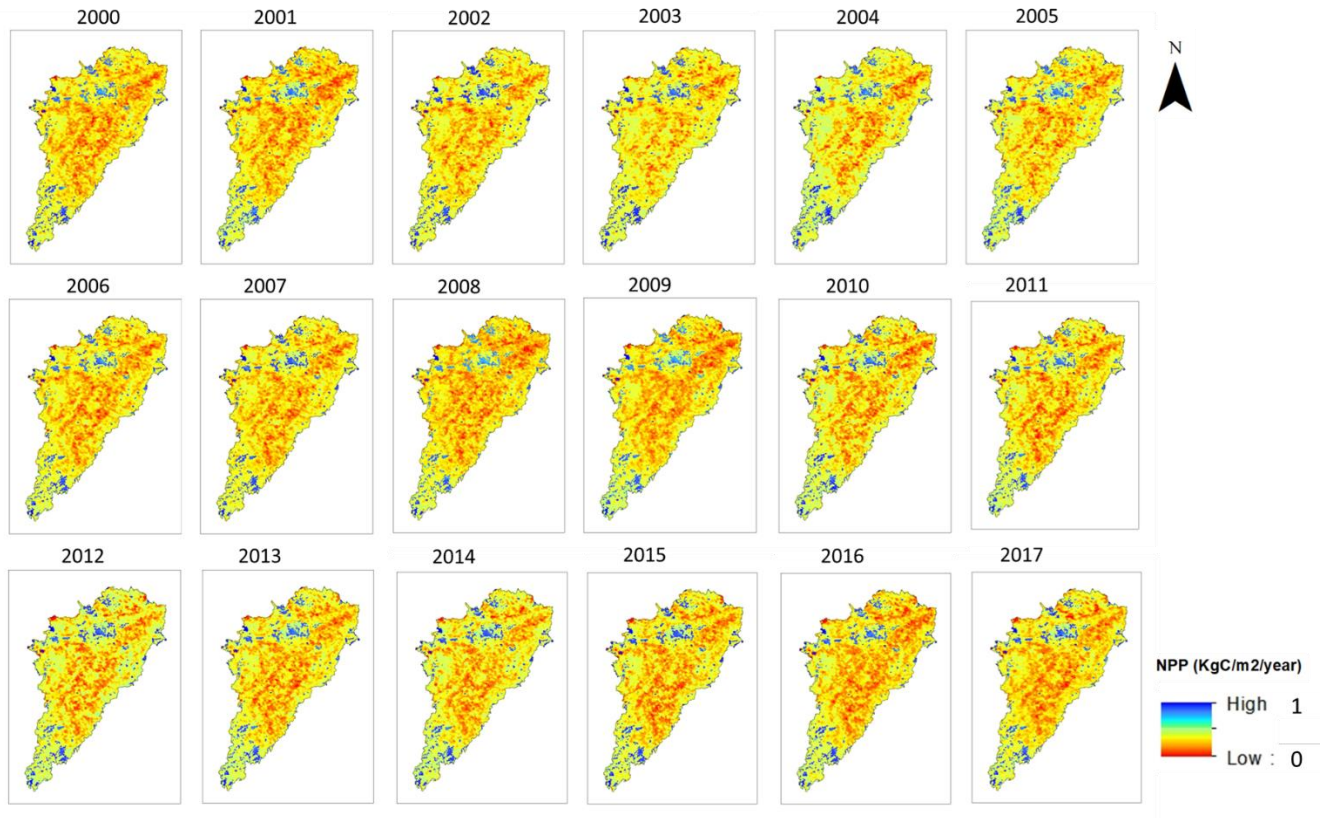

Figure 4A. Tile drainage distribution across the South Nation watershed (data provided by the South Nation Conservation Authority).

760

Figure 5A: Net Primary Productivity (NPP) data for SNW (based on MODIS data (Endsley et al., 2023))